NASA TECHNICAL NOTE

NASA TN D-2998

LOW-SPEED FORCE AND FLIGHT INVESTIGATION OF VARIOUS METHODS FOR CONTROLLING PARAWINGS

by Joseph L. Johnson, Jr.

Langley Research Center
Langley Station, Hampton, Va.

NATIONAL AERONAUTICS AND SPACE ADMINISTRATION - WASHINGTON, D. C. - DECEMBER 1965

LOW-SPEED FORCE AND FLIGHT INVESTIGATION OF VARIOUS METHODS FOR CONTROLLING PARAWINGS

By Joseph L. Johnson, Jr.

Langley Research Center
Langley Station, Hampton, Va.

Technical Film Supplement L-882 available on request

NATIONAL AERONAUTICS AND SPACE ADMINISTRATION

For sale by the Clearinghouse for Federal Scientific and Technical Information
Springfield, Virginia 22151 – Price $2.00

LOW-SPEED FORCE AND FLIGHT INVESTIGATION OF VARIOUS METHODS FOR CONTROLLING PARAWINGS

By Joseph L. Johnson, Jr.
Langley Research Center

SUMMARY

A preliminary low-speed, wind-tunnel investigation has been made to study various methods of controlling parawings. Force tests were first made with a simple model to study various methods of control. Some of the control systems which appeared promising on the basis of the force-test results were evaluated under dynamic conditions in a flight-test investigation of a model of a parawing utility vehicle. The study was initiated because the center-of-gravity shift used as a control system on some parawing configurations has resulted in relatively large stick forces and unstable stick-force gradients, inertia feedback problems, and poor lateral control effectiveness under some conditions of flight.

The results of the investigation indicated that such devices as horizontal control surfaces, trailing-edge boltropes, trailing-edge risers, and hinged wing tips offered enough promise for providing a satisfactory means of controlling parawings to warrant further consideration. The particular control device best suited for a given parawing configuration, however, will probably depend to a large extent on both the type of application and the particular handling-qualities requirements set forth for that application.

INTRODUCTION

In a general research program being conducted by the National Aeronautics and Space Administration to provide some basic information on configurations employing the parawing concept, a low-speed force- and flight-test investigation has been conducted to study various methods of controlling parawings. This study was undertaken because the results of several experimental and analytical studies, such as those of references 1 to 4, have shown that the center-of-gravity shift used as a control system on most configurations to date may lead to relatively large control forces and poor control effectiveness for some applications under certain conditions of flight. The present investigation was conducted with a simplified model for the force tests and with the model used in reference 1 for the flight tests. Both models had a leading-edge sweep of 50° and had leading-edge and keel members of equal length.

Force tests were made to study the static stability and control characteristics of the simplified model with several different control systems. Some of the control systems that appeared promising on the basis of the force-test results with the simple model were evaluated under dynamic conditions on the flight-test model. A few static force tests were also made with the flight-test model to obtain stability and control information for direct correlation with the flight-test results.

Motion pictures were taken to evaluate the model behavior during parts of the flight tests. A request form for this film supplement is included at the back of this report.

SYMBOLS

All forces, moments, and velocities with the exception of lift and drag are presented with respect to a system of body axes originating at the reference center-of-gravity positions shown in figures 1 to 4. For the force-test model, this reference system of axes coincided approximately with the parawing keel, whereas for the flight-test model, it was near the platform of the model. Measurements for this investigation were taken in the U.S. Customary System of Units. Equivalent values are indicated herein parenthetically in the International System (SI) in the interest of promoting use of this system in future NASA reports. Details concerning the use of SI, together with physical constants and conversion factors, are given in reference 5. All measurements are reduced to standard coefficient form and are based on the dimensional characteristics of the flat-pattern sweep of the wing (45° leading-edge sweep).

X,Y,Z	longitudinal, lateral, and normal body axes, respectively
x,z	distances along X- and Z-body axes, feet (meters)
S	wing area, feet^2 (meters^2)
b	wing span, feet (meters)
l_k	keel length, feet (meters)
V	free-stream velocity, feet per second (meters per second)
q	free-stream dynamic pressure, pounds force per square foot (newtons per square meter)
α_k	angle of attack of keel, degrees
α_p	angle of attack of platform, degrees
i_t	angle of incidence of horizontal tail measured from keel axis, positive trailing edge down, degrees

i_w	angle of incidence of parawing keel angle with respect to platform, $\alpha_k - \alpha_p$, degrees
β	angle of sideslip, $-\psi$, degrees
ϵ	downwash angle, degrees
ψ	angle of yaw, degrees
ϕ	angle of roll, positive right wing tip down, degrees
δ_e	deflection of elevator surface, positive trailing edge down, degrees
δ_t	deflection of hinged wing tips, positive trailing edge down, degrees
F_L	lift, pounds force (newtons)
F_D	drag, pounds force (newtons)
L/D	lift-drag ratio
F_X	axial force, pounds force (newtons)
F_Y	side force, pounds force (newtons)
H	hinge moment, positive (positive when M_H tends to deflect keel trailing edge downward or wing-tip trailing edge outward), foot-pounds force (meter-newtons)
M_H	hinge moment, foot-pounds force (meter-newtons)
M_Y	pitching moment, foot-pounds force (meter-newtons)
M_X	rolling moment, foot-pounds force (meter-newtons)
M_Z	yawing moment, foot-pounds force (meter-newtons)
C_L	lift coefficient, F_L/qS
C_D	drag coefficient, F_D/qS
C_Y	lateral-force coefficient, F_Y/qS
C_m	pitching-moment coefficient, M_Y/qSl_k
C_n	yawing-moment coefficient, M_Z/qSb

C_l rolling-moment coefficient, M_X/qSb

$\Delta C_Y, \Delta C_n, \Delta C_l, \Delta C_h, \Delta C_m$ incremental force and moment coefficient

S_t tail area, square foot (meter^2)

C_h hinge-moment coefficient, H/qSl_k or H/qSb

$C_{Y_\beta} = \frac{\partial C_Y}{\partial \beta}$, per degree

$C_{n_\beta} = \frac{\partial C_n}{\partial \beta}$, per degree

$C_{l_\beta} = \frac{\partial C_l}{\partial \beta}$, per degree

$C_{m_{i_t}} = \frac{\partial C_m}{\partial i_t}$, per degree

Subscripts:

k keel

p platform or wing pivot point

MODELS AND APPARATUS

The force-test model used in the investigation was constructed of three aluminum tubes of equal length (0.0125 keel length in diameter) which were attached together at the nose to form the apex of the parawing. A sweep angle of 50° was maintained by a spreader bar which was attached both to the leading edges and to the keel at approximately the 35-percent keel station. The fabric used to form the membrane of the parawing consisted of a nonporous Mylar film bonded to a nylon ripstop parachute cloth.

Several modifications were made to the parawing force-test model to allow for various control studies. Included in these modifications were hinged wing-tip and keel members, a trailing-edge boltrope, trailing-edge risers, and horizontal control surfaces. The hinged wing tips had a chord of 17 percent of the leading-edge length and were designed so that they could be deflected in several different planes. These planes varied from that which coincided with the plane of the leading edges and keel to those which coincided with planes approximately parallel for one case and perpendicular in another to the wing-fabric contour near the tips. The location of the hinged tips, trailing-edge boltrope, and trailing-edge risers used in the tests are shown in figure 2. The trailing-edge boltrope and trailing-edge risers were designed so that they could be

shortened or lengthened to alter the trailing-edge shape of the wing for control. A sketch showing the horizontal tails and horizontal control surface used on the model is shown in figure 3.

The flight-test model used in the investigation was the same model as that tested in the investigation reported in reference 1 and consisted basically of a platform attached to a parawing by means of an overhead truss arrangement. (See fig. 4.) A detailed description of the flight-test model is given in reference 1. Dimensional and mass characteristics of the model are given in table I. In the previous investigation, this model was controlled by banking and pitching the wing with respect to the platform. In the present investigation, however, the wing was locked in pitch and bank relative to the platform, and control was provided by other means. For most flights, longitudinal control was obtained through symmetrical deflection of the hinged wing tips, although a few flights were made in which the boltrope was used for pitch control. Roll control was achieved through differential deflection of the hinged wing tips and directional control was provided through a rudder mounted directly in the propeller slipstream. Power for the flight-test vehicle was supplied by a pneumatic motor driving a four-blade pusher propeller. Sketches of the flight-test model showing the wing-tip control system and boltrope control system used on the model are presented in figures 5(a) and 5(b), respectively.

For all flight tests, the wing tips were deflected in a plane which coincided with the plane of the leading edges and keel. The chord of the hinged wing tips on the flight model was 25 percent of the keel length.

The flight tests were conducted in the Langley full-scale tunnel. A complete description of the flight-test technique used in the tests is given in reference 6, and the technique and equipment are illustrated in figure 6. Static force tests of the flight model were made in the Langley full-scale tunnel. The force-test model was tested in a low-speed wind tunnel with a 12-foot octagonal test section at the Langley Research Center. Sting-type support equipment and strain-gage balances were used in the force tests.

TESTS

Force Tests

The force-test model was tested over an angle-of-attack range of the parawing keel from 10° to 45° to determine the longitudinal and lateral control characteristics of the model with various control devices installed. The control devices investigated included hinged wing tips, hinged keel trailing-edge member, horizontal control surfaces located at the aft end of the model, trailing-edge boltrope and trailing-edge risers. These tests were made at a dynamic pressure of about 1.0 pound per square foot (47.88 N/m^2) which corresponds to an airspeed of about 29 feet per second (8.84 m/sec) and to a Reynolds number based on the parawing keel length of 0.91×10^6.

Force tests were made on the flight model to obtain static stability and control information for direct correlation with the flight-test results. All force tests for this model were made with power off. The tests were made over an angle-of-attack range of the model platform from -10° to 20° for a wing incidence condition of 20°. (The wing was locked in pitch at this angle of incidence for all tests.) Control devices used in the force tests on the flight model included hinged wing tips (which were deflected symmetrically for pitch control and differentially for roll control) and a trailing-edge boltrope. The model with hinged wing tips was tested for a range of control-deflection angles from ±5° to ±15°. All force tests on the flight model were made at a dynamic pressure of about 1.2 pounds per square foot (57.46 N/m^2), which corresponds to an airspeed of about 32 feet per second (9.75 m/sec) at standard sea-level conditions and to a test Reynolds number of about 1.65×10^6 based on the parawing keel length of 8.0 feet (2.4 m).

Flight Tests

Flight tests were made to study the dynamic stability and control characteristics of the flight-test model over an angle-of-attack range of the parawing keel from about 23° to 38°. For most flights, longitudinal control was obtained through symmetrical deflection of the hinged wing tips. Roll control was achieved through differential deflection of the hinged wing tips, and directional control was provided through a rudder mounted directly in the propeller slipstream. For a few tests, a boltrope was used to provide longitudinal control by changing the length of the boltrope from its neutral position. Wing-tip deflection angles of ±5° were used for pitch and roll control and a rudder deflection angle of ±10° was used for yaw control.

For most flights, the longitudinal position of the center of gravity was 1.7 inches (4.32 cm) rearward and 6.2 inches (15.75 cm) above the force-test center-of-gravity reference shown in figure 4. For the flight-test center-of-gravity position, longitudinal trim was achieved by changing the trim setting of the wing tips; however, at angles of attack above about 35°, it was necessary to shift the center of gravity slightly rearward in order to achieve trim.

RESULTS AND DISCUSSION

Static Longitudinal Control Characteristics of Force-Test Model

Hinged keel tip.- The results of the tests with the hinged keel tip used for pitch control are presented in figure 7. These data show that control deflections of 10° from neutral produced relatively large incremental changes in lift, drag, and pitching moment, but that the effectiveness decreased considerably for higher deflections. An upward deflection from neutral produced the desired changes in pitching moment but caused excessive flutter in the fabric, particularly at the lower angles of attack. For this reason, this type of control may have very limited application on configurations which have parawings with negative values of $C_{m,o}$ (such as the test model). Before such a

device can be made practical, it appears that some means of providing a positive $C_{m,o}$ is needed in order to allow an initial downward deflection of the parawing trailing edge as a neutral condition. A deflection of the trailing edge upward to its normal contour from this neutral (down) condition would then give the desired increment of nose-up control or trim without leading to excessive flutter.

Hinged wing tips.- The results of tests with the hinged wing tips used for pitch control are presented in figure 8. These data show that tip deflections produced incremental pitching-moment changes but a comparison of the data of figures 7 and 8 indicates that for a given deflection, the wing tips were not as effective in producing pitching moment as the keel tip. Deflection of the leading edges inward for up control produced the desired changes in pitching moment but caused excessive flutter in the fabric trailing edge. This problem in combination with the negative value of $C_{m,o}$ of the parawing may limit the usefulness of the wing-tip control for pitch in much the same manner as that pointed out previously for the keel tip control.

Trailing-edge risers and boltrope.- The results of tests to determine the pitch effectiveness of trailing-edge risers and a trailing-edge boltrope are presented in figures 9 and 10, respectively. The data of figures 9(a) and 9(b) indicate that incremental pitching moments can be produced by shortening various riser combinations at the parawing trailing edge, but the variation in moments with deflection is not as linear as that produced by boltrope deflection as indicated by a comparison of the data of figure 9 with those of figure 10. The data of figure 10 are in agreement with the results of other boltrope studies, such as that of reference 7, and show that shortening the length of the boltrope for control produced relatively large changes in pitching moment. As in the cases of the other devices tested, some means of providing a positive $C_{m,o}$ is needed when boltrope or riser deflection is used for pitch control in order to allow some initial downward deflection to be used as a neutral condition before these control systems can become practical. A low center of gravity provides a positive value of $C_{m,o}$ of the complete vehicle, but the magnitude of this $C_{m,o}$ and the effectiveness of the boltrope or riser control systems would depend on the particular configuration involved.

Horizontal control surfaces.- The results of tests to determine the pitch effectiveness of two different horizontal tails and a horizontal control surface mounted near the rear of the wing are presented in figures 11(a) to 11(c). The data of figures 11(a) and 11(b) indicate that the small horizontal tail $\left(S_t/S = 0.025\right)$ was ineffective for pitch control, but that the larger tail $\left(S_t/S = 0.08\right)$ provided a considerable increase in pitch effectiveness. The data of figure 11(c) show that a control surface with both an increase in aspect ratio and size (see fig. 3(b)) provided an even greater increase in pitch effectiveness. Presented in figure 12 is a plot of the downwash angle against angle of attack for the large tail below the parawing and for the horizontal control surface mounted to the keel; the results indicate that in the angle-of-attack region between 20° and 30°, the downwash factor $(1 - d\epsilon/d\alpha)$ is near that experienced by conventional horizontal tails behind conventional wings. The data of figure 13 summarize the pitch-effectiveness information for

the three horizontal surfaces studied and show, as pointed out previously, that the surface mounted between the keel and leading edges provided the highest control effectiveness. The effectiveness for this surface, however, is not as high in comparison with that of the other configurations as might have been expected on the basis of its relative size and aspect ratio. This result can probably be attributed to the fact that the moment arm for this surface is shorter than that for the tail in the position below the keel.

Static Lateral Control Characteristics of Force-Test Model

Keel-tip deflection.- The incremental lateral forces and moment coefficients produced by lateral deflection of the keel trailing edge are presented in figure 14. The results of these tests show that the keel tip was fairly effective for producing rolling moments at the lower angles of attack, but that, as the angle of attack increased, the rolling-moment increments ΔC_l decreased while the yawing-moment increments ΔC_n due to deflection became adverse and increased to values about equal to those of the favorable rolling moments.

In connection with the keel control tests, it was observed that considerable luffing occurred in the side of the parawing trailing edge that became unloaded as the hinged keel control moved to the right or left. This luffing seemed to be more severe than that which occurred with wing-tip deflection.

Hinged wing tips.- The incremental lateral force and moment coefficients produced by wing-tip deflection are presented in figure 15. The results of these tests show that for the three conditions studied, deflecting the tips in the plane of the keel and leading edges (inward and outward) produced the highest rolling moments and also produced favorable yawing moments at angles of attack up to about 35° and very little adverse yawing moment at higher angles of attack. Deflection of the tips in the plane of the fabric at the tip section produced relatively high values of rolling moments and produced yawing moments that were about zero at low angles of attack and slightly favorable at the higher angles of attack. The least effective condition of those investigated, as far as rolling moments are concerned, was the deflection of the tips perpendicular to the canopy at the tip section, but this condition produced fairly large favorable yawing moments over the angle-of-attack range.

Boltrope and riser deflection.- The results of tests to determine the lateral effectiveness of boltrope and riser control systems are presented in figure 16. The results in this figure show that these control systems provided relatively high rolling effectiveness at the lower angles of attack but as the angle of attack increased the incremental rolling moments decreased and the yawing moments, which were adverse, became large. The effectiveness of the riser control system increased with the number of risers used. With three risers deflected on each side the canopy shape was very similar to that with the boltrope deflected and, as might be expected, the effectiveness of this system appeared to be very similar to that of the boltrope system.

Horizontal control surface.- The lateral forces and moments produced by differential deflection of the horizontal control surface mounted between the keel and leading edges of the force-test model (fig. 3(b)) are presented in figures 17(a) and 17(b). These data indicate that this control surface provided relatively large rolling moments over the angle-of-attack range investigated but that the yawing moments due to control deflection were adverse and became nearly as large as the rolling moments at the highest angles of attack. One significant observation to be made about this control system is that it appears to provide relatively large rolling moments which could probably be achieved with relatively low hinge moments, but that it would add weight and complexity to the aft portion of the parawing and may not be practical.

Control Characteristics of Flight-Test Model With Hinged Wing Tips

Static longitudinal control.- The results of tests to determine the longitudinal control effectiveness of hinged wing tips on the flight-test model are presented in figure 18. The results of these tests show that the tips were considerably more effective in producing incremental pitching moments for the flight model than for the force-test model. (See fig. 7.) The primary reason for this increase in effectiveness is the fact that the chord of the tips was greater for the flight model (25 percent of the keel length for the flight model as compared with 17 percent for the force-test model).

At the time of the force and flight tests on the flight model the hinge moments of the wing-tip control system were not measured. Since the time of these tests, however, a considerable amount of work concerning wing-tip and keel-tip hinge-moment information has been published (for example, in refs. 2 and 4). Some of these data are presented in figure 19 together with the results of the present study for comparison purposes. The plot at the top of figure 19 shows that the incremental pitching moment produced by a given deflection varied in direct proportion to the increase in control length and that the keel-tip deflection was more effective in this respect than the wing tips. At the bottom of figure 19 the incremental hinge moment is presented as a function of control length. Analysis indicates that these hinge moments should increase approximately as the square of the increase in control length. The curves shown were faired according to this relationship and the data for the wing-tip control appear to substantiate this analysis.

A plot of incremental pitching moment against incremental hinge moment (presented in fig. 20) for the wing-tip and keel-tip control systems indicates that the keel-tip control system provided considerably more pitching moment for a given value of hinge moment than that of the wing-tip control system. Also presented in figure 20 is the hinge-moment and pitching-moment relationship for center-of-gravity-shift control systems for two values of vertical center-of-gravity position below the parawing keel. A comparison of this information for the center-of-gravity shift and wing-tip control systems shows that the center-of-gravity-shift system was the less effective for a value z/l_k of 0.25, which is approximately that of the present flight-test model. For the value of z/l_k of 0.50 the two control systems were very similar in

terms of the hinge moment required to produce a given incremental pitching moment.

Static lateral control.- The results of tests to determine the lateral control effectiveness of wing-tip controls on the flight model are presented in figure 21. For these tests, the tips were deflected inward and outward in the plane of the leading edges and keel. The data of figure 21(c) show that the incremental rolling moments due to tip deflection generally increased with increasing angle of attack and that the yawing moments due to tip deflection were favorable over most of the angle-of-attack range investigated. At low angles of attack ($\alpha_p = -10^\circ$) where the fabric was luffing, the tips were ineffective for control. The hinge moments, as expected, increased with increasing deflection and with increasing angle of attack.

As pointed out previously, the initial tests made with the wing-tip control system did not include hinge-moment studies. The hinge-moment data were obtained in subsequent tests and are included in this paper to provide a more thorough evaluation of the wing-tip control system. A summary of this information is presented in figures 22 to 25. Comparable data from references 2, 4, and 7 are included.

From the plot presented at the upper part of figure 22, it can be seen that the incremental rolling moment produced by tip deflection varied roughly in direct proportion to the increase in tip length (as noted earlier in connection with pitching-moment data). The lower plots of figure 22 show the variation of the incremental hinge moment resulting from tip deflection as a function of the ratio of control length to leading-edge length for two different ranges of values of this ratio. The dashed curve in these lower plots represents the variation of hinge moment with control length assuming that the hinge moments increased as the square of the increase in control length. This curve is seen to intersect the test points for the small control lengths as well as for the full leading-edge control. It appears therefore that the assumed variation is substantiated very well by test data.

The results presented in figure 23 show the relationship between the net rolling moment (rolling moment at zero yawing moment) and the hinge moment for the various configurations investigated. It is necessary to consider the net rolling moment in this comparison because there are yawing moments involved with tip deflection which, by causing the model to sideslip, can increase or decrease the rolling effectiveness of the control system because of the rolling moment due to sideslip. An explanation of this effect is given in reference 2. The data of figure 23 show that the effectiveness for wing-tip control as well as for wing-bank control varied considerably from one configuration to another. The reason for this variation in effectiveness for any given control system can be attributed to a large extent to the fact that each of the configurations involved had parawings of different overall geometry and of different construction.

For the vehicles under consideration, the highest rolling moment produced for a given hinge moment was achieved in the modified utility vehicle of reference 4. In this configuration the wing-tip controls had relatively small chords (14 percent keel length) and were deflected in the plane of the parawing fabric

at the tip section. In the vehicle of reference 2 (full-size flexible-wing utility vehicle) and in the flight-test model of the present investigation, the wing-tip controls were of approximately 25 percent of the keel in length and were deflected inward and outward in the plane of the leading edges and keel. Although there is considerable difference in the effectiveness of the wing-tip control system for the configurations involved, it is significant to point out that all of the configurations showed much higher rolling moments for a given hinge moment when the wing-tip control system was used than when the wing-bank system was used.

Presented in figure 24 is a plot of the ratio of $\Delta C_l/\Delta C_h$ against the ratio of control length to leading-edge length for the configurations discussed in figures 22 and 23. The symbols plotted in figure 24 represent the ratios of $\Delta C_l/\Delta C_h$ for the three configurations with wing-tip control presented in figure 23. The ratios of $\Delta C_l/\Delta C_h$ in these cases are net rolling-moment values and are higher than those shown by the solid line (which came from the data of figure 22) because of the fact that favorable yaw was produced with tip deflection and this yawing produced additional favorable rolling moments through the effective dihedral parameter C_{l_β}. The dotted lines in figure 24 represent the spread in the ratio of $\Delta C_l/\Delta C_h$ for the wing-bank control presented in figure 23. From the information presented in figure 24 it appears that for wing-tip control to show some advantage over wing-bank control it is necessary, at least for some configurations, to keep the length of the tip controls less than about 30 percent of the leading-edge length.

One other significant point concerning the results presented in figure 24 is that parawings generally have a reduction in C_{n_β} and L/D at high angles of attack and these changes could alter considerably the net rolling moment produced by wing bank. The results shown in figure 24 represent the angle-of-attack condition near maximum L/D ($\alpha = 25^\circ$) where the ratio of $\frac{C_{l_\beta}}{C_{n_\beta}\ L/D}$ is at a minimum and therefore the control effectiveness of the wing-bank control system is likely to be at a maximum. In order to illustrate the change in effectiveness of the wing-bank control system with increasing angle of attack, values of $C_{l,net}$ were computed for the three configurations discussed in figures 23 and 24, and the results are presented in figure 25. The data of figure 25 show that for the three configurations under consideration, a rapid reduction occurred in $C_{l,net}$ at an angle of attack near 30° and at an angle of attack near 35° the wing-bank control system became ineffective.

Flight Tests

The model behavior during flight was observed by the pitch pilot located at the side of the test section and by the roll-yaw pilot located at the rear of the test section. The results obtained in the flight tests were primarily in the form of qualitative ratings of flight behavior based on the opinions of

these pilots. Motion-picture records obtained in the tests were used to verify and correlate the ratings for the different tests of the model, and some of this film has been prepared as a film supplement to this report and is available on loan. A request card form and a description of the film are found at the back of this report.

Longitudinal stability and control.- The dynamic longitudinal stability characteristics of the model were generally similar to those reported in reference 1 - that is, the model was dynamically stable over the angle-of-attack range investigated (keel angles from 23° to 38°). The longitudinal motions appeared to be well damped throughout the angle-of-attack range investigated including the stall.

The longitudinal control provided by symmetrical deflection of the wing tips was considered generally satisfactory for pitch control at the lower and moderate angles of attack investigated. In this angle-of-attack range, the wing tips provided enough control to overcome disturbances and to maneuver and position the model in the tunnel satisfactorily. At the higher angles of attack (above about 30°) the maneuver capability provided by the control system deteriorated and the response of the model to control became somewhat sluggish. This deterioration in control response was believed to be partly a result of the fact that the tips were trimmed inward to provide nose-up trim at the higher angles of attack and the pitching effectiveness of the tips was reduced somewhat from that for a trim setting of zero degrees (see fig. 18). Other factors which might also account for this deterioration in response are the increase in static margin and also, perhaps, an increase in pitch damping at the higher angles of attack.

It should be pointed out in connection with the use of wing-tip deflection for pitch control that the hinge moments associated with this control system can become large when the length of the control arms is relatively long. In the flight-test model, the control arms were 25 percent of the keel length and, based on the data of figure 22, the hinge moments in pitch in this case were appreciable and increased with deflection and with angle of attack. No consideration was given to the hinge moments in the model flight tests but it is obvious that the hinge moments as well as the pitching moments produced by the wing tips must be taken into consideration in comparing the relative merits of this control system with those of other systems envisioned for controlling parawings in pitch.

In addition to the tests in which the wing-tip control system was used, a few tests were also made in which a boltrope was used to provide pitch control. These tests were made for an angle-of-attack range from 25° to 30° and showed that with enough change in length (±1.5 inches on the model) the boltrope system provided adequate control for satisfactorily overcoming disturbances and for maneuvering the model. The response to boltrope deflection was fairly rapid and little effort was required by the pilot in recovering the model from fairly large disturbances within the limited area of the test section.

Lateral stability and control.- The lateral stability characteristics of the model were similar to those reported in reference 1 in that the model was

found to be directionally stable and the lateral oscillations were well damped over the angle-of-attack range of the tests.

Deflecting the wing tips alone for lateral control provided a satisfactory means of controlling the model over an angle-of-attack range from about 23° to 32° but this control became progressively weaker as the angle of attack was increased above about 32°. In the lower angle-of-attack range, the model could be maneuvered and positioned quite well and recovered easily from large disturbances within the limited area of the tunnel test section. It was found that the wing tips alone provided lateral control which was about as good as that provided by coordinated wing-tip and rudder control and better than that provided by rudder alone.

As the angle of attack was increased above about 32°, however, the control provided by the wing tips became progressively weaker and, although sustained flights could be made up to about 38° angle of attack under relatively undisturbed conditions, the control was considered inadequate for maneuvering and for satisfactorily recovering the model from large disturbances. This deterioration in control effectiveness of the wing tips at high angles of attack is apparently related to the fact that the yawing moments produced by tip deflection decreased from favorable values at low and moderate angles of attack to zero or adverse values at the higher angles of attack. The static control data of figure 21(c) indicate that the yawing moments produced by control deflection should not have decreased to zero until about 40° angle of attack. The difference in the static and flight control data can probably be attributed to the fact that at the higher angles of attack the tips were trimmed inward to provide nose-up trim and the lateral control effectiveness of the tips might have been reduced somewhat from that indicated by the data of figure 21(c) for a trim setting of zero degrees.

In flight tests with the rudder coordinated to deflect with the wing tips, it was found that satisfactory lateral control was provided over the entire angle-of-attack range. It was also found that, because of the high values of effective dihedral at the higher angles of attack, the model could be flown satisfactorily with the rudder alone in this range. This result is similar to that reported in reference 1 for rudder-alone control.

A comparison of the results of this investigation with those in which the model was flown with wing-bank control (see ref. 1) indicates that in the lower angle-of-attack range (below about 25°) the two systems were about equally effective in providing satisfactory lateral control. As the angle of attack was increased above about 25° the control provided by wing bank became progressively weaker and at about 35° angle of attack became ineffective and sustained flights could not be made. On the basis of these results it appears therefore that at the higher angles of attack the wing-tip controls were somewhat more effective for lateral control than wing-bank control in that sustained flights could be made for angles of attack through 38° despite a reduction in control effectiveness. In connection with this comparison, it was found in another investigation (ref. 4) that wing-tip control provided satisfactory lateral control (without the use of a rudder) at high angles of attack when it was employed differently. In the investigation of reference 4 the tips were deflected in the

plane of the fabric at the tip section rather than inward and outward in the plane of the leading edges and keel as in the case of the present model.

CONCLUDING REMARKS

The results of force- and flight-test investigations to study various methods of controlling parawings indicated that such devices as horizontal control surfaces, a trailing-edge boltrope, trailing-edge risers, and hinged wing tips offered enough promise for providing a satisfactory means of controlling parawings to warrant further consideration. The particular control device best suited for a given parawing configuration, however, will probably depend to a large extent on both the type of application and the particular handling-qualities requirements set forth for that particular application.

Langley Research Center,
National Aeronautics and Space Administration,
Langley Station, Hampton, Va., September 1, 1965.

REFERENCES

1. Johnson, Joseph L., Jr.: Low-Speed Wind-Tunnel Investigation to Determine the Flight Characteristics of a Model of a Parawing Utility Vehicle. NASA TN D-1255, 1962.

2. Johnson, Joseph L., Jr.; and Hassell, James L., Jr.: Full-Scale Wind-Tunnel Investigation of a Flexible-Wing Manned Test Vehicle. NASA TN D-1946, 1963.

3. Landgraf, F.; Everett, W. L.; and Burich, J. H.: Flexible-Wing Manned Test Vehicle. TCREC Tech. Rep. 62-25 (Ryan Rep. 61B131A), U.S. Army Transportation Res. Command (Fort Eustis, Va.), June 25, 1962.

4. Johnson, Joseph L., Jr.: Low-Speed Force and Flight Investigation of a Model of a Modified Parawing Utility Vehicle. NASA TN D-2492, 1965.

5. Mechtly, E. A.: The International System of Units - Physical Constants and Conversion Factors. NASA SP-7012, 1964.

6. Paulson, John W.; and Shanks, Robert E.: Investigation of Low-Subsonic Flight Characteristics of a Model of a Hypersonic Boost-Glide Configuration Having a 78° Delta Wing. NASA TN D-894, 1961.

7. Naeseth, Rodger L.; and Gainer, Thomas G.: Low-Speed Investigation of the Effects of Wing Sweep on the Aerodynamic Characteristics of Parawings Having Equal-Length Leading Edges and Keel. NASA TN D-1957, 1963.

TABLE I.- DIMENSIONAL AND MASS CHARACTERISTICS OF THE MODELS

Force-Test Model

Parawing dimensions:		
Area (developed, 45° leading-edge sweep)	16.95 sq ft	(1.575 m^2)
Span (based on 45° leading-edge sweep)	6.92 ft	(2.11 m)
Keel length	4.90 ft	(1.50 m)
Horizontal-tail dimensions:		
Small horizontal tail -		
Area	0.424 sq ft	(0.0394 m^2)
Span	1.125 ft	(0.343 m)
Chord	0.376 ft	(0.115 m)
Large horizontal tail -		
Area	1.600 sq ft	(0.149 m^2)
Span	2.250 ft	(0.686 m)
Chord	0.710 ft	(0.216 m)
Horizontal control surface mounted to keel and leading-edge member -		
Area (one panel only)	1.272 sq ft	(0.118 m^2)
Span (one panel only)	3.000 ft	(0.914 m)
Chord	0.424 ft	(0.129 m)

Flight-Test Model

Weight	39.0 lb	(173.48 N)
Wing loading	0.863 lb/sq ft	(41.32 N/m^2)
Parawing dimensions:		
Area (developed, 45° leading-edge sweep)	45.30 sq ft	(4.21 m^2)
Span (based on 45° leading-edge sweep)	11.32 ft	(3.45 m)
Keel length	8.0 ft	(2.44 m)
Rudder dimensions:		
Area	0.834 sq ft	(0.077 m^2)
Span	1.43 ft	(0.436 m)
Chord	0.584 ft	(0.178 m)

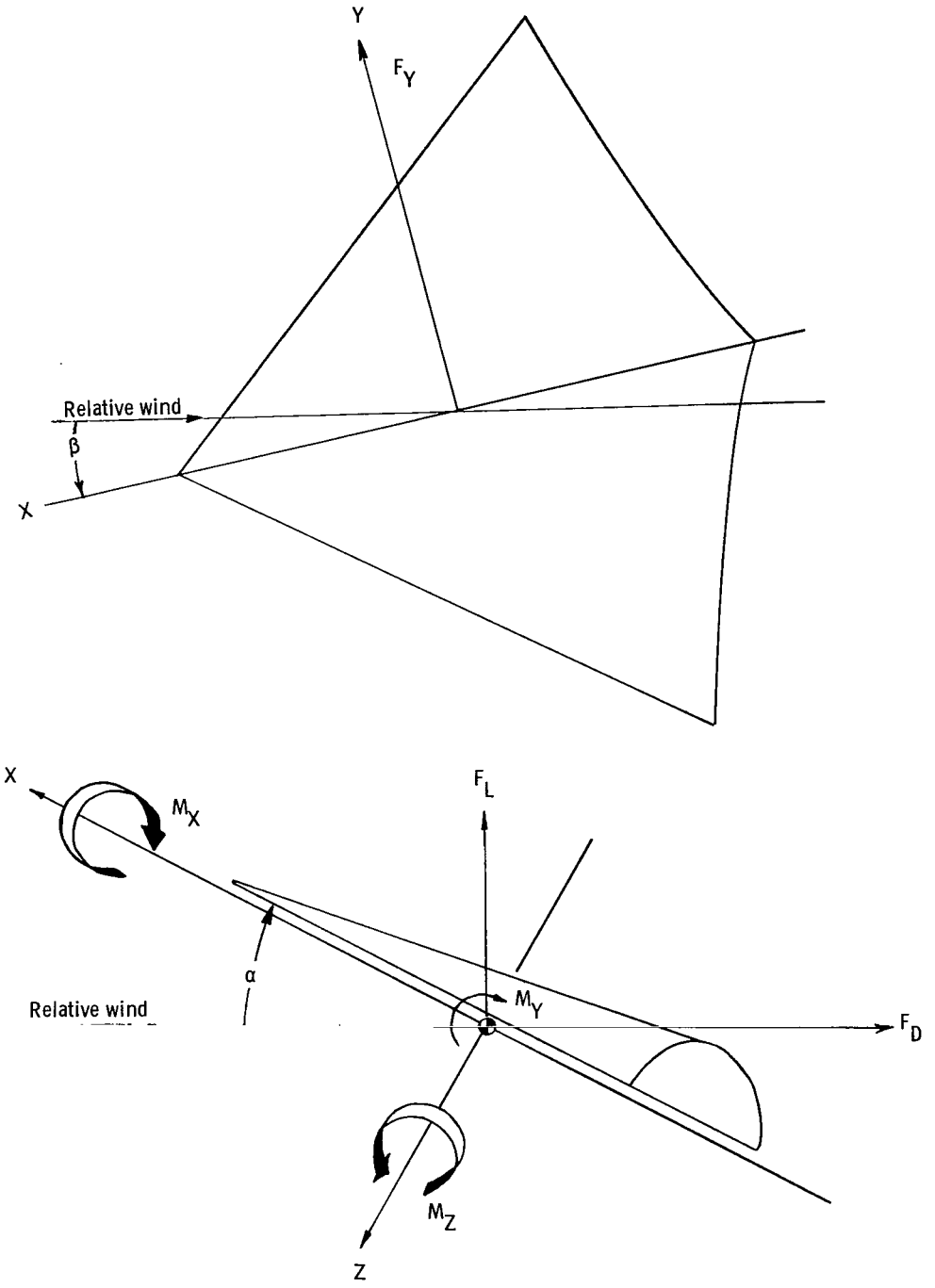

Figure 1.- System of axes used in the investigation for the force-test model. The longitudinal data are referred to wind axes and the lateral data are referred to body axes. Arrows indicate positive direction of moments, forces, and angles.

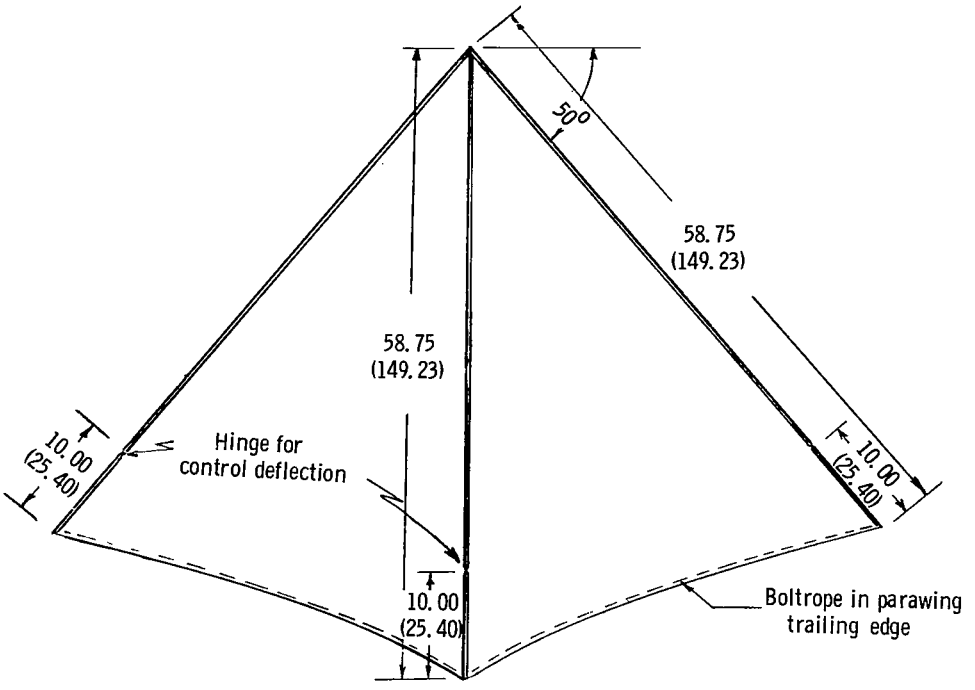

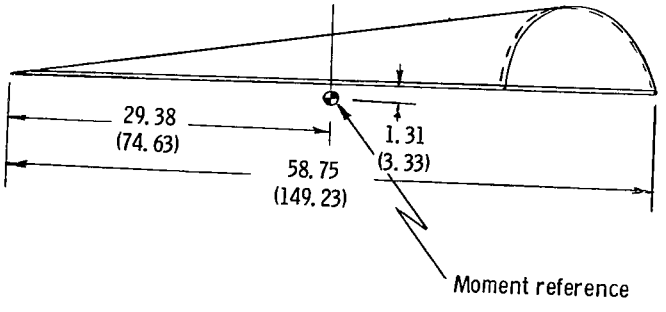

(a) Hinge-tip and keel-tip arrangement.

Figure 2.- Sketch of parawing force-test model. Dimensions are indicated first in inches and parenthetically in centimeters.

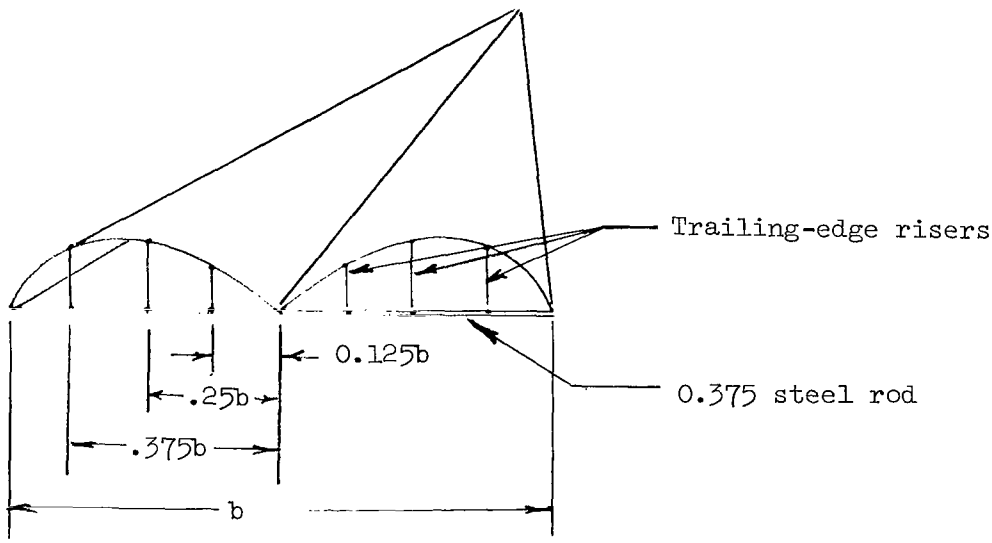

(b) Trailing-edge riser arrangement.

Figure 2.- Concluded.

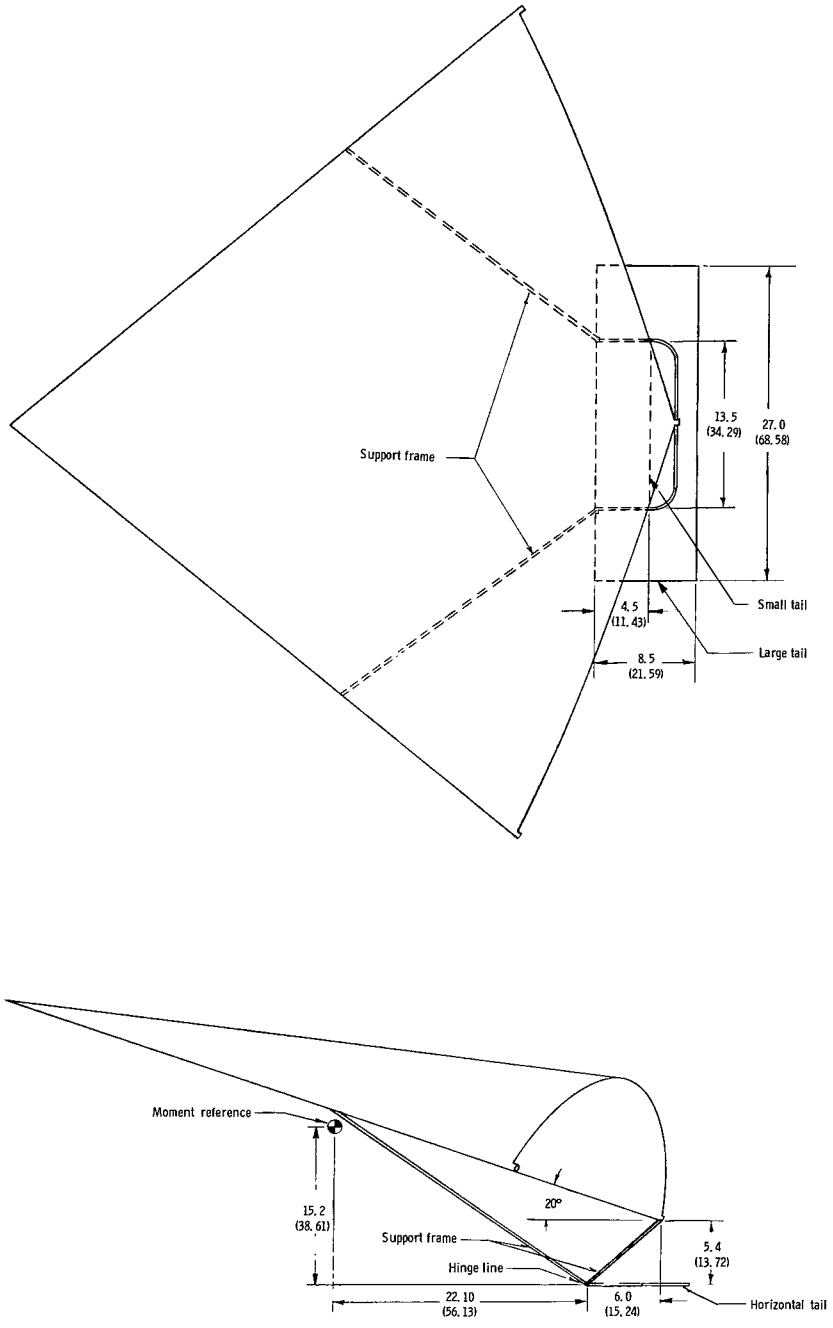

(a) Horizontal tails.

Figure 3.- Sketch of parawing force-test model with horizontal-tail arrangement and horizontal control surface used in the tests. Dimensions are given first in inches and parenthetically in centimeters.

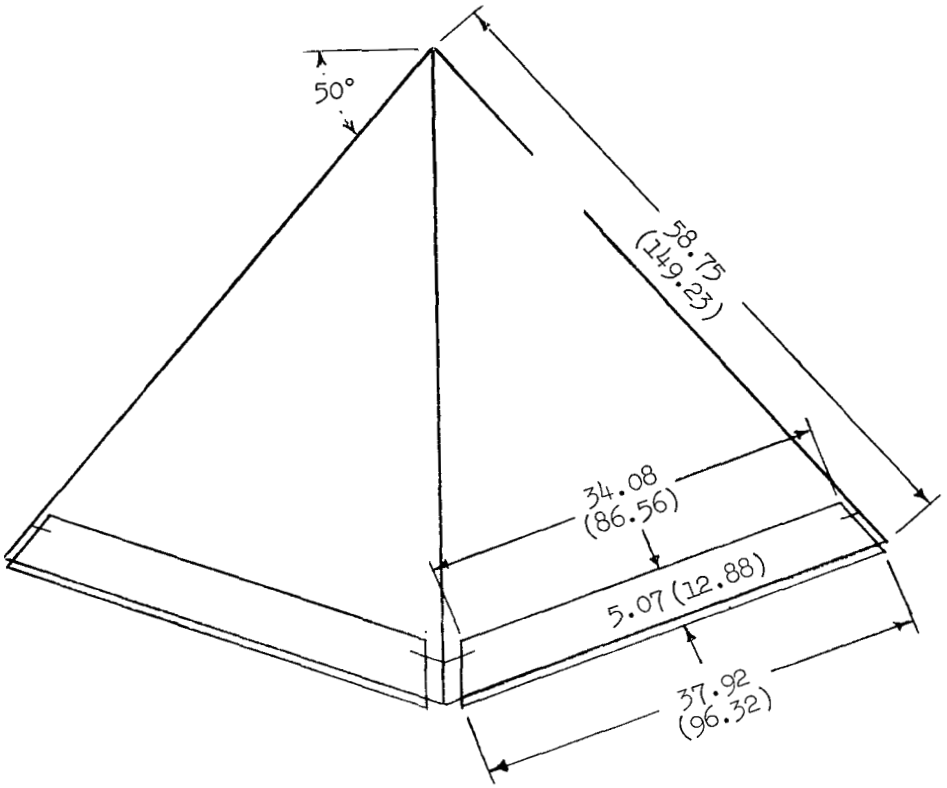

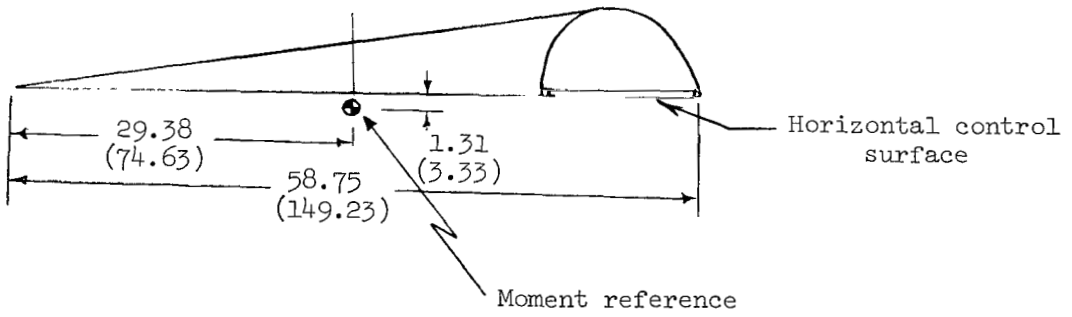

(b) Horizontal control surface.

Figure 3.- Concluded.

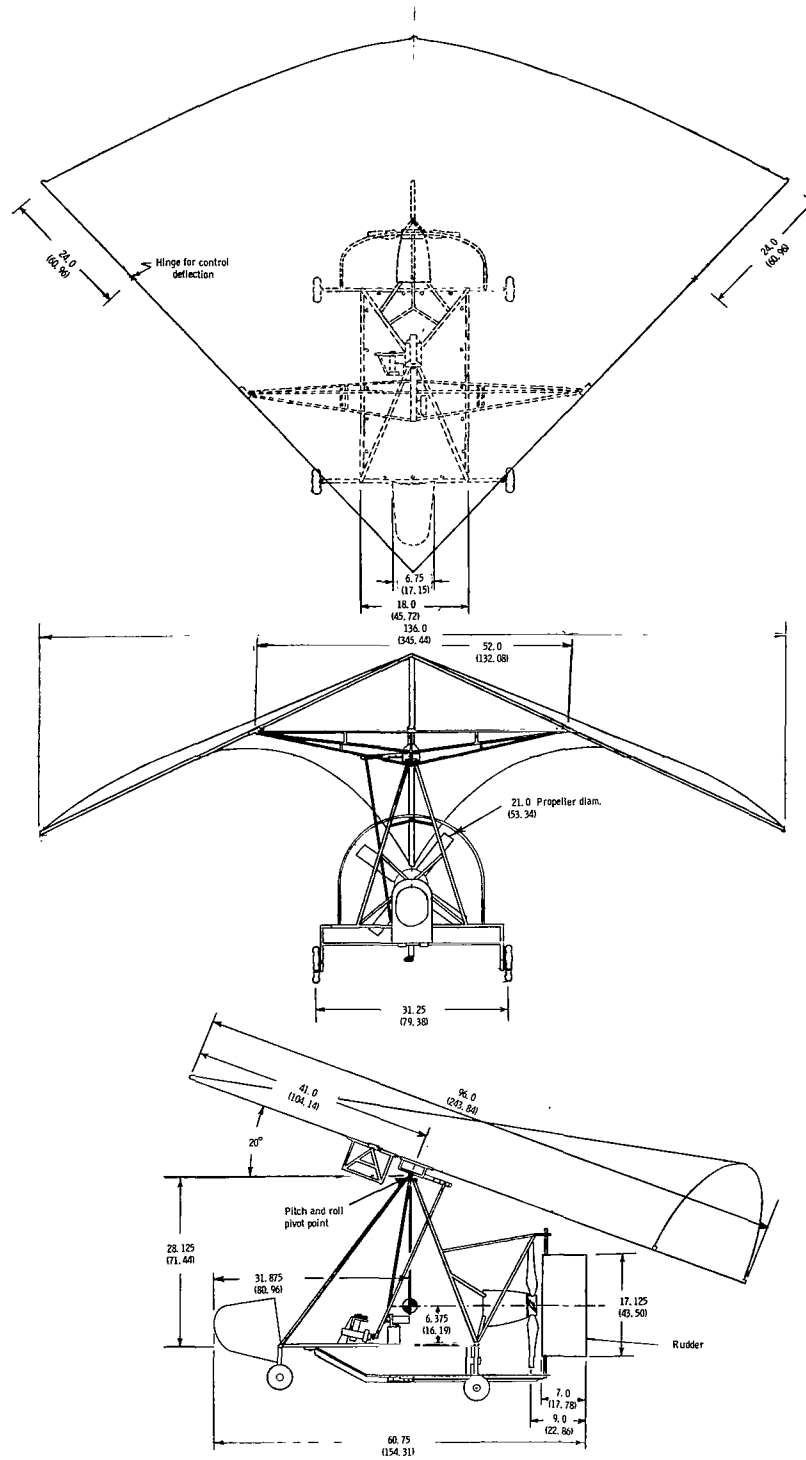

Figure 4.- Three-view drawing of flight-test model. Dimensions are given first in inches and parenthetically in centimeters.

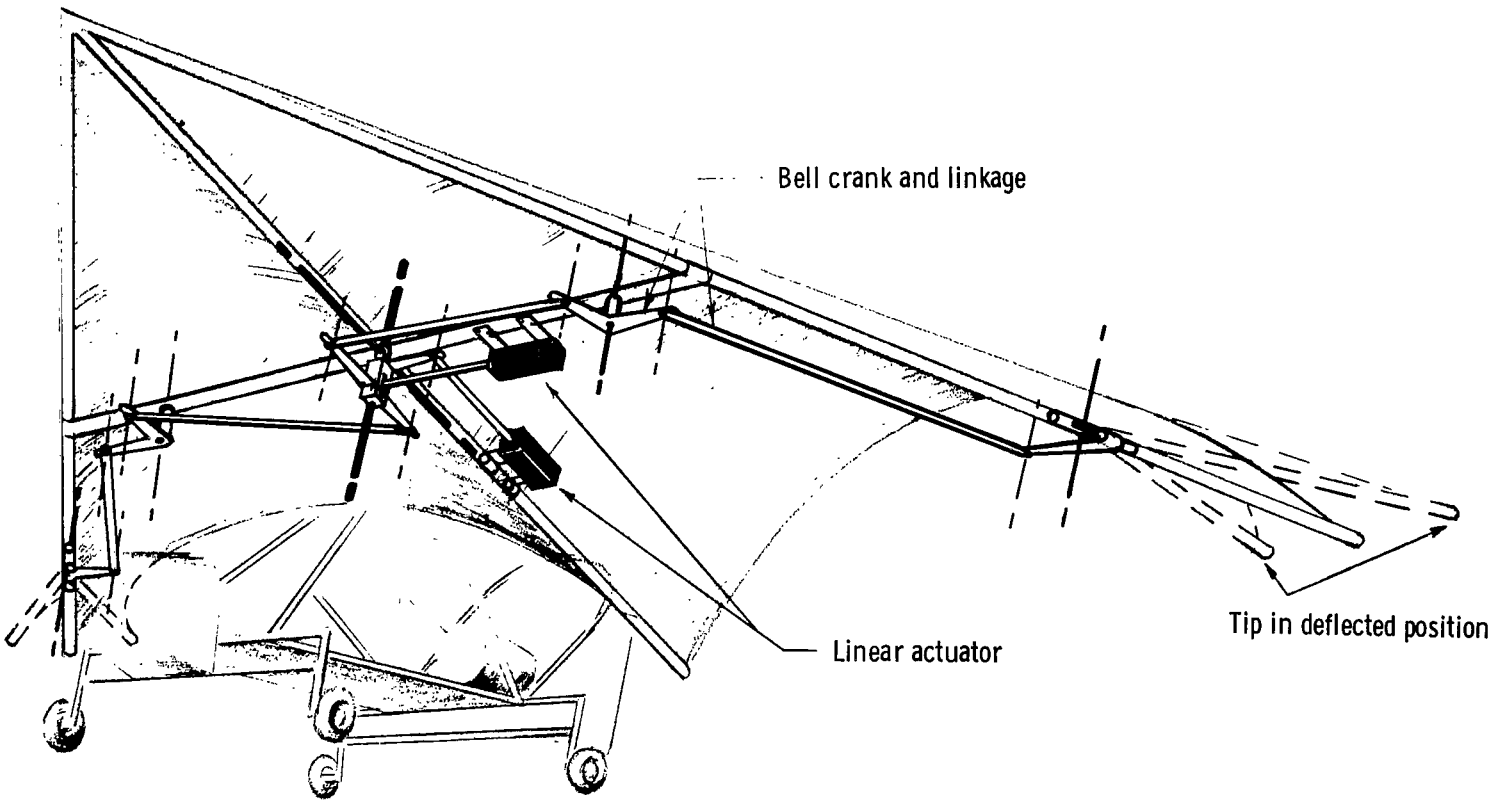

(a) Wing-tip control.

Figure 5.- Detailed drawing of the control system used on the flight-test model.

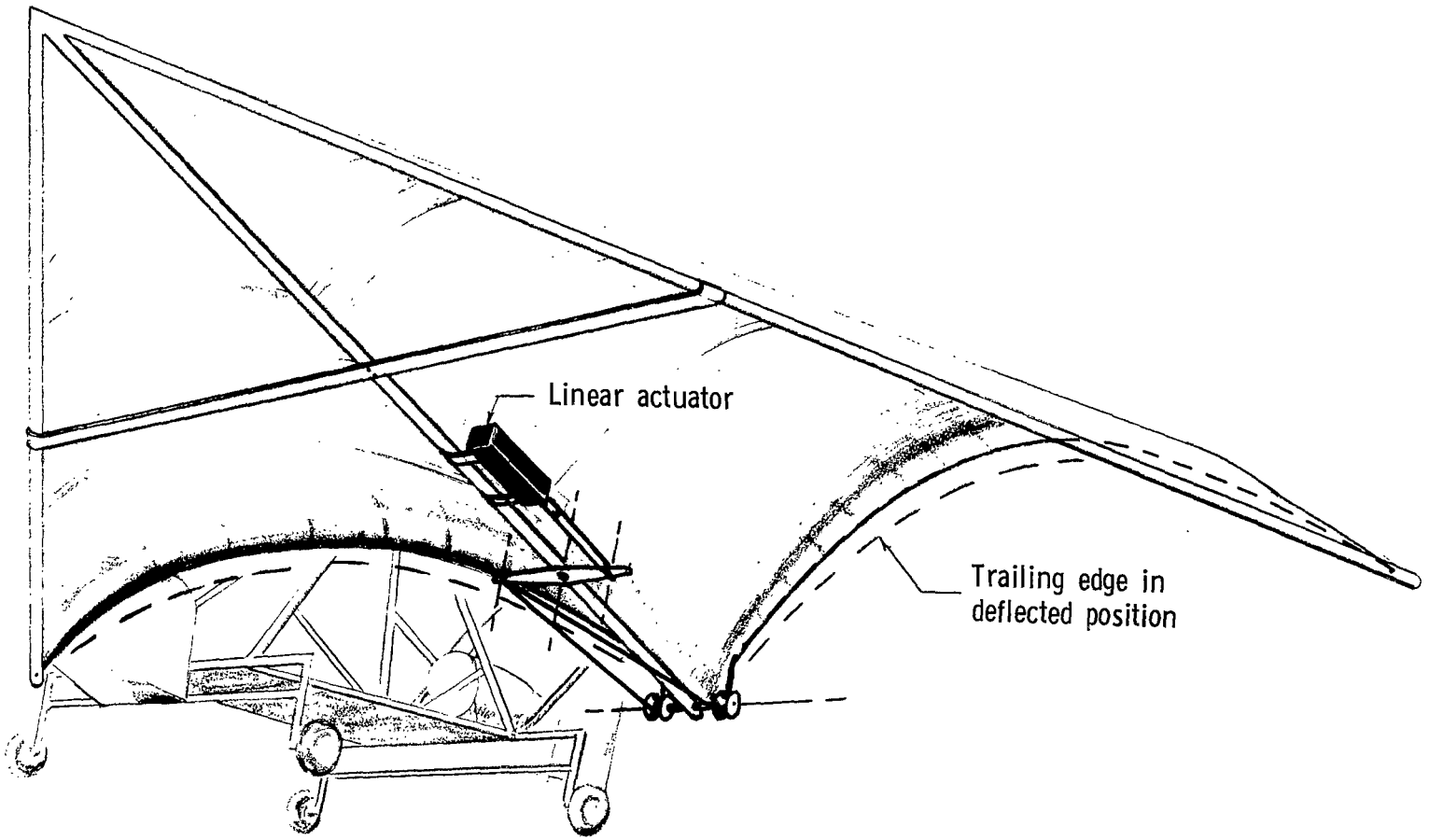

(b) Boltrope control.

Figure 5.- Concluded.

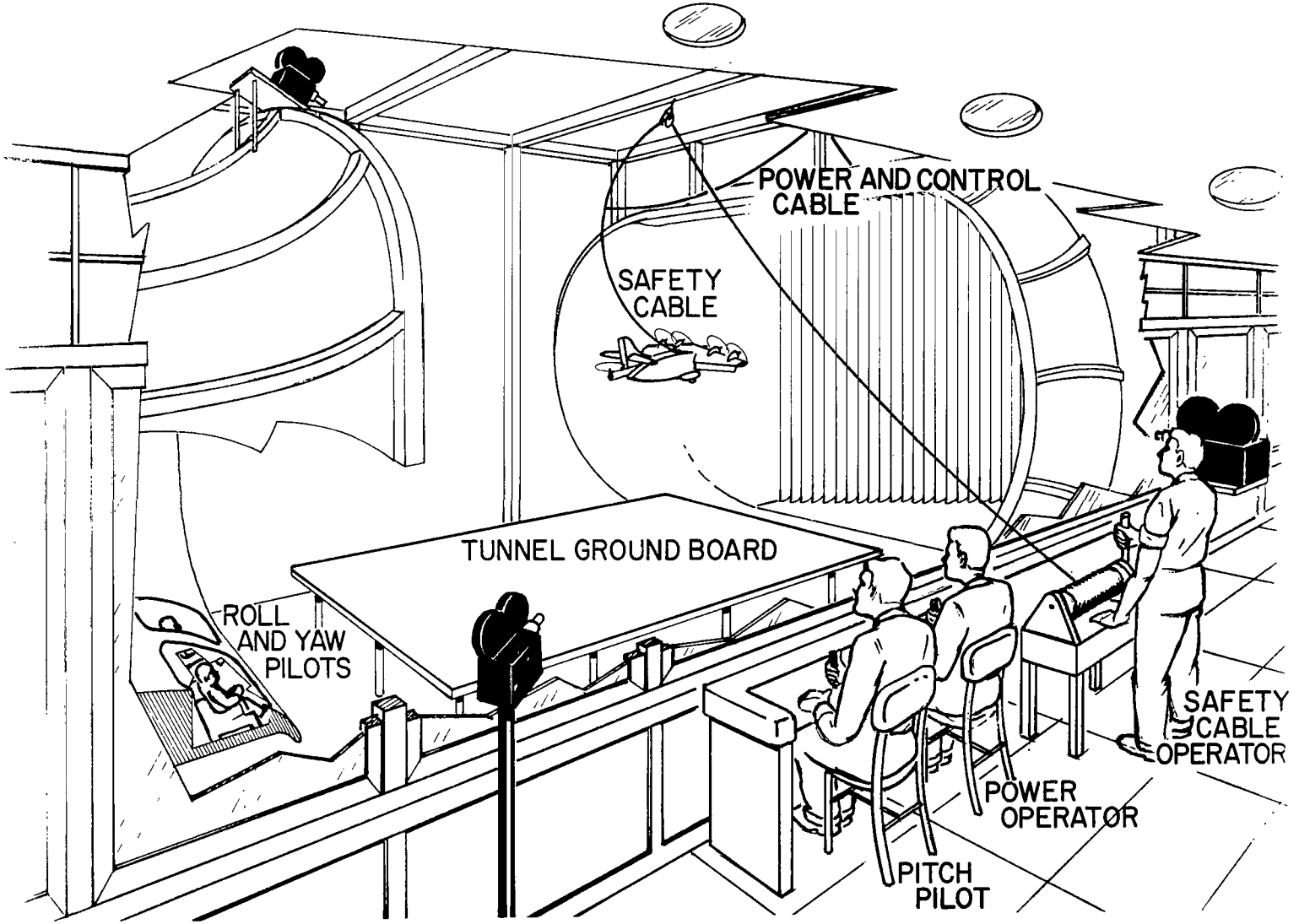

Figure 6.- Sketch of flight-test setup in the Langley full-scale tunnel.

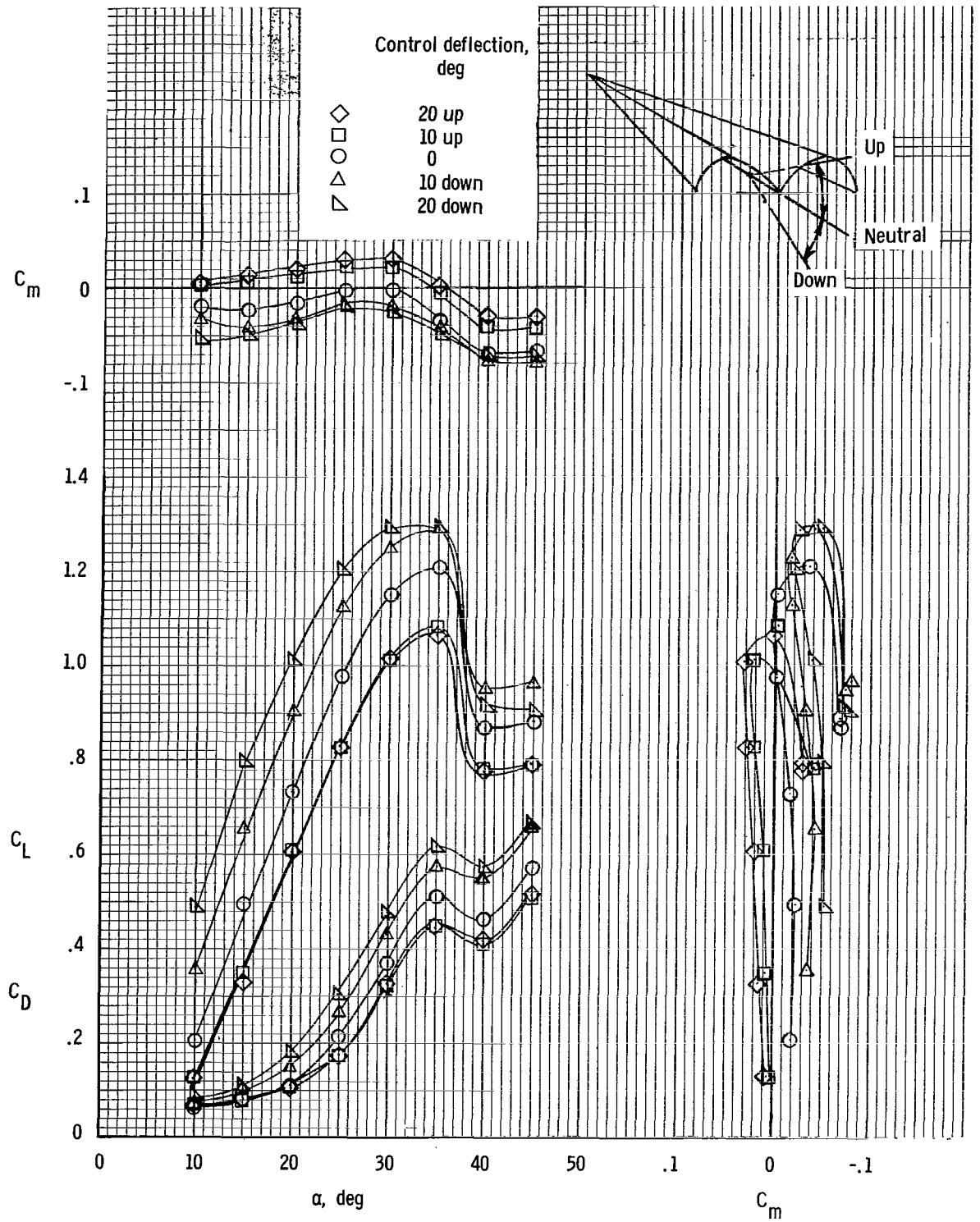

Figure 7.- Pitch effectiveness of keel control system. Force-test model.

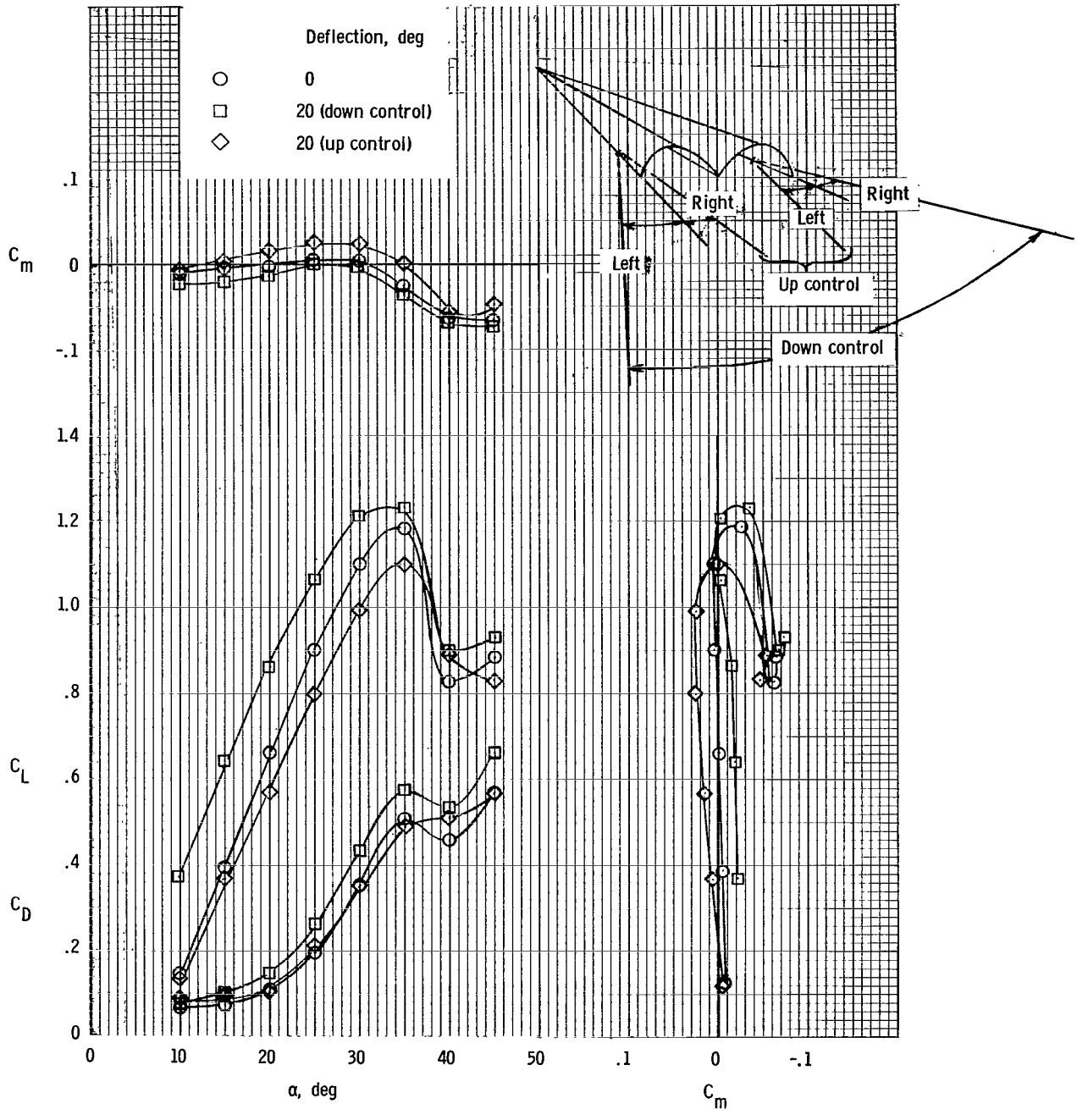

Figure 8.- Pitch effectiveness of wing tips. Force-test model. (Tips deflected in horizontal plane, inward for up control, outward for down control.)

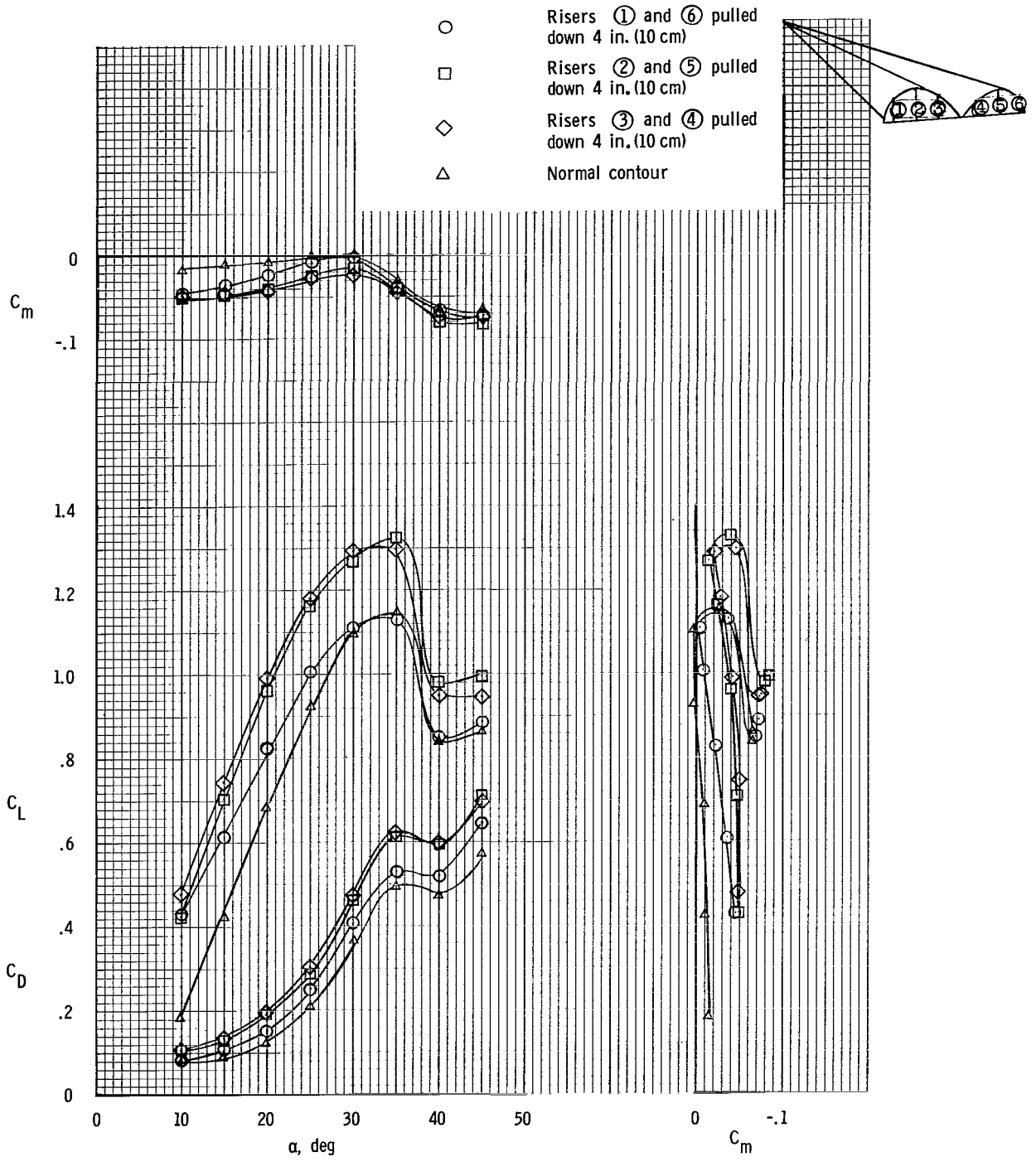

(a) Individual riser deflection.

Figure 9.- Pitch effectiveness of trailing-edge risers. Force-test model.

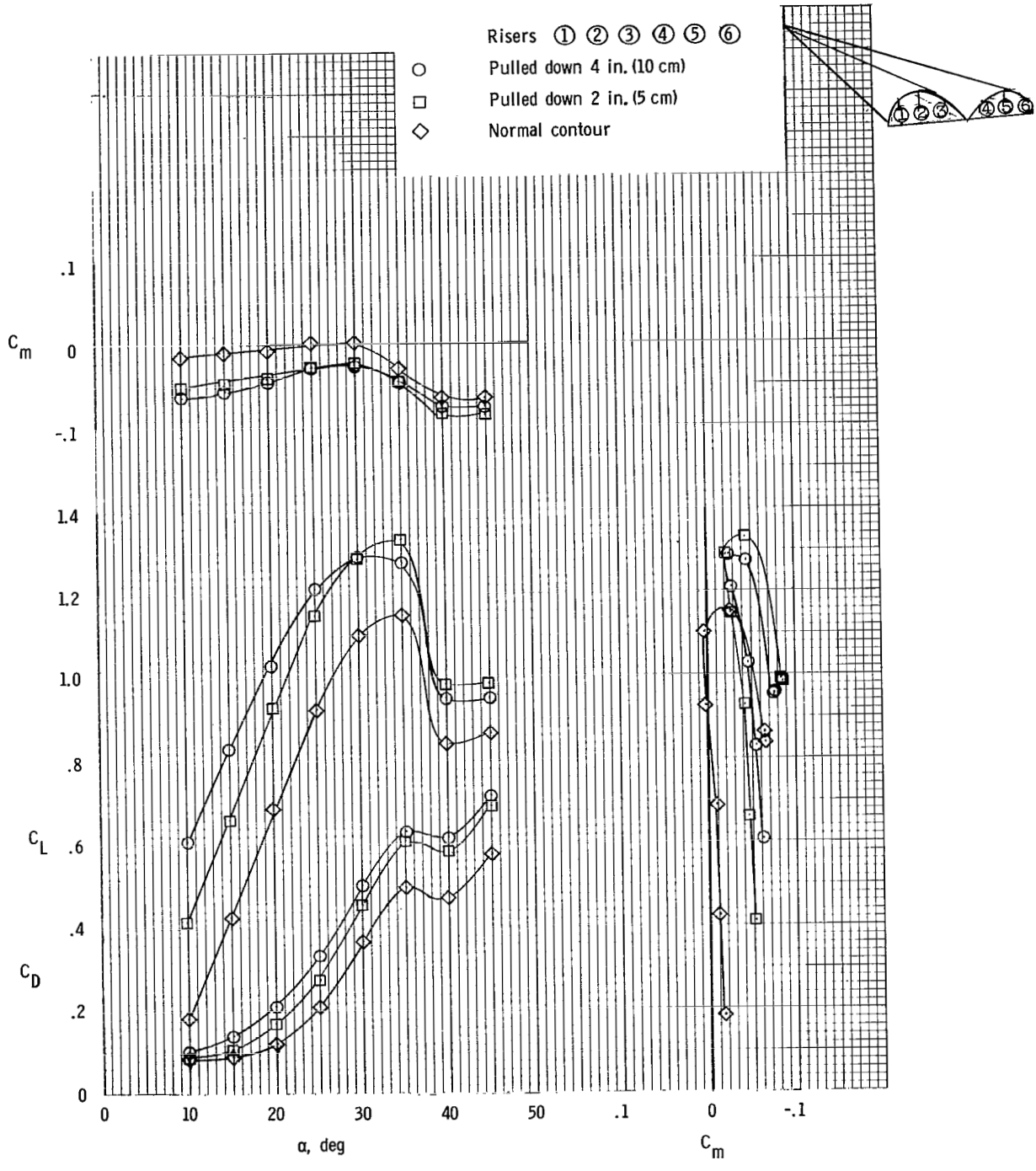

(b) Total riser deflection.

Figure 9.- Concluded.

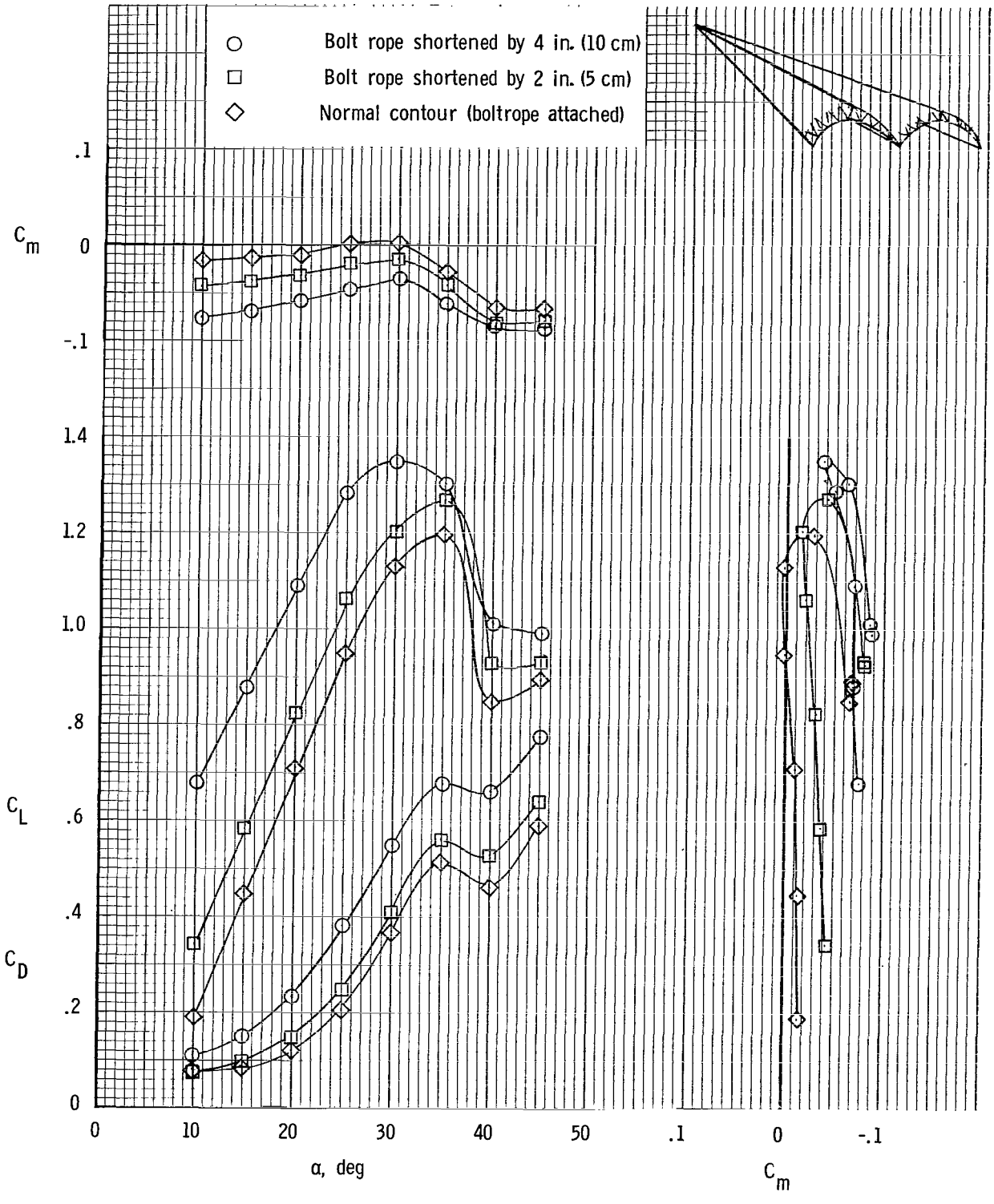

Figure 10.- Pitch effectiveness of boltrope control system. Force-test model.

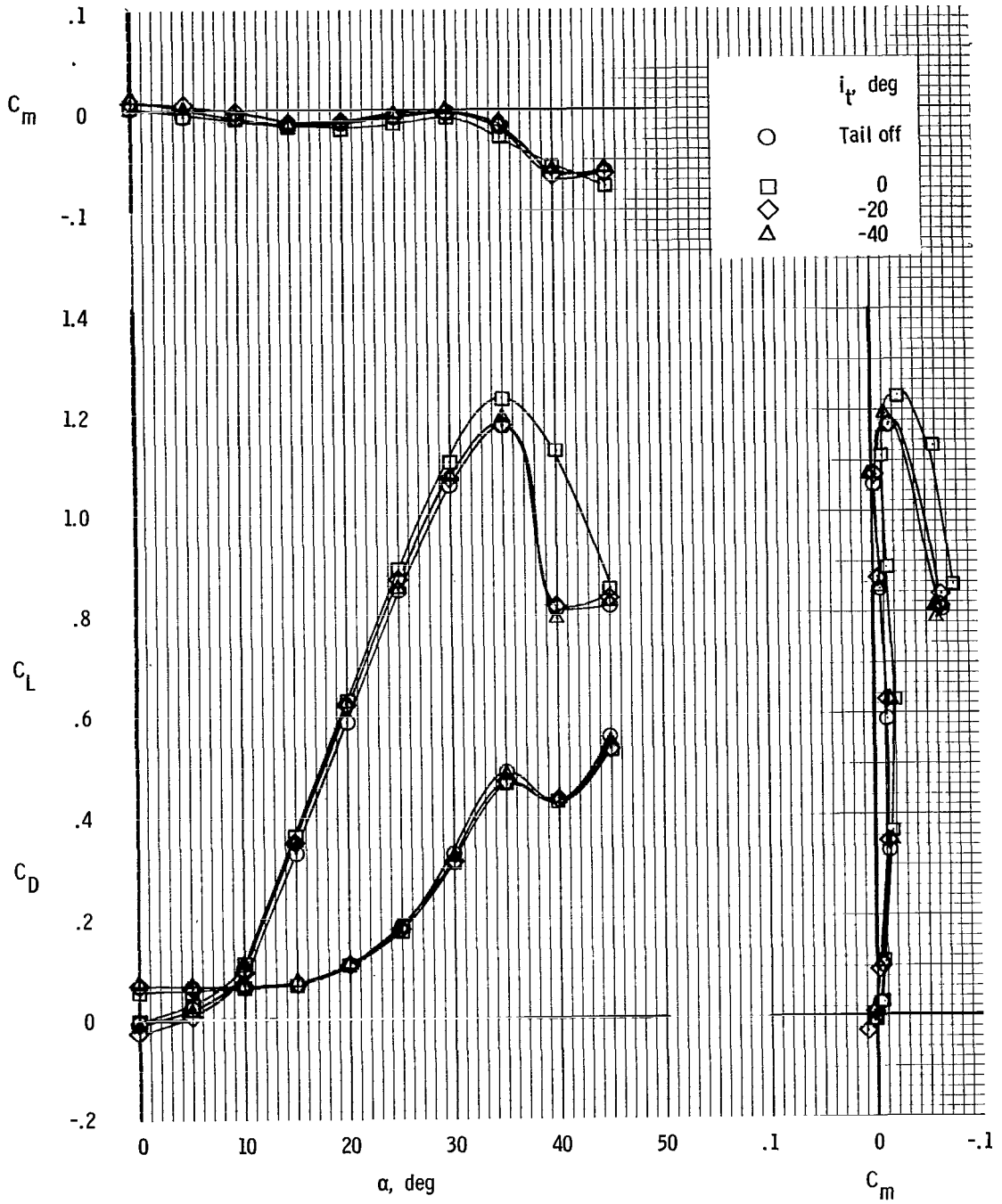

(a) Small horizontal tail.

Figure 11.- Pitch effectiveness of horizontal-tail arrangements and horizontal control surface. Force-test model.

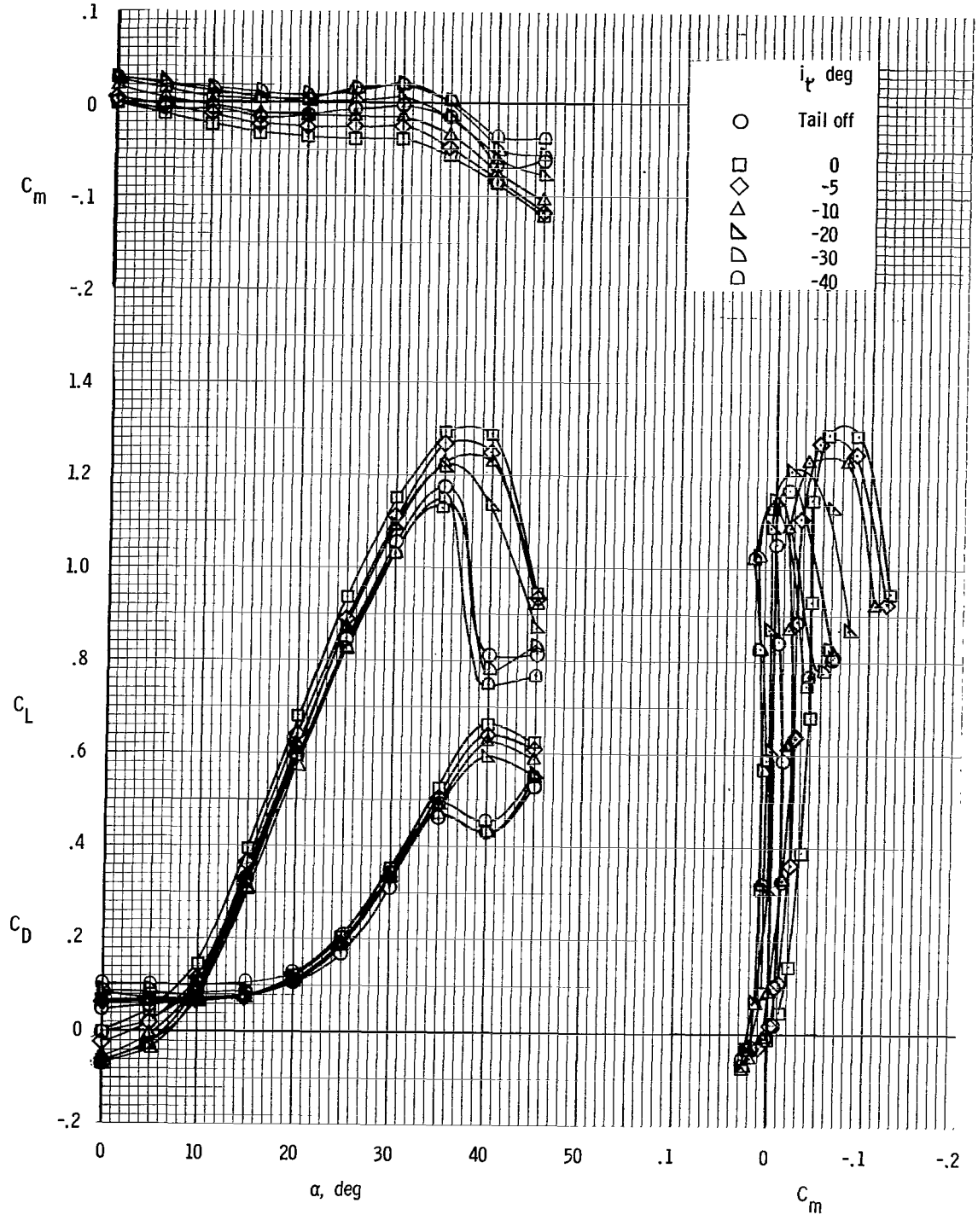

(b) Large horizontal tail.

Figure 11.- Continued.

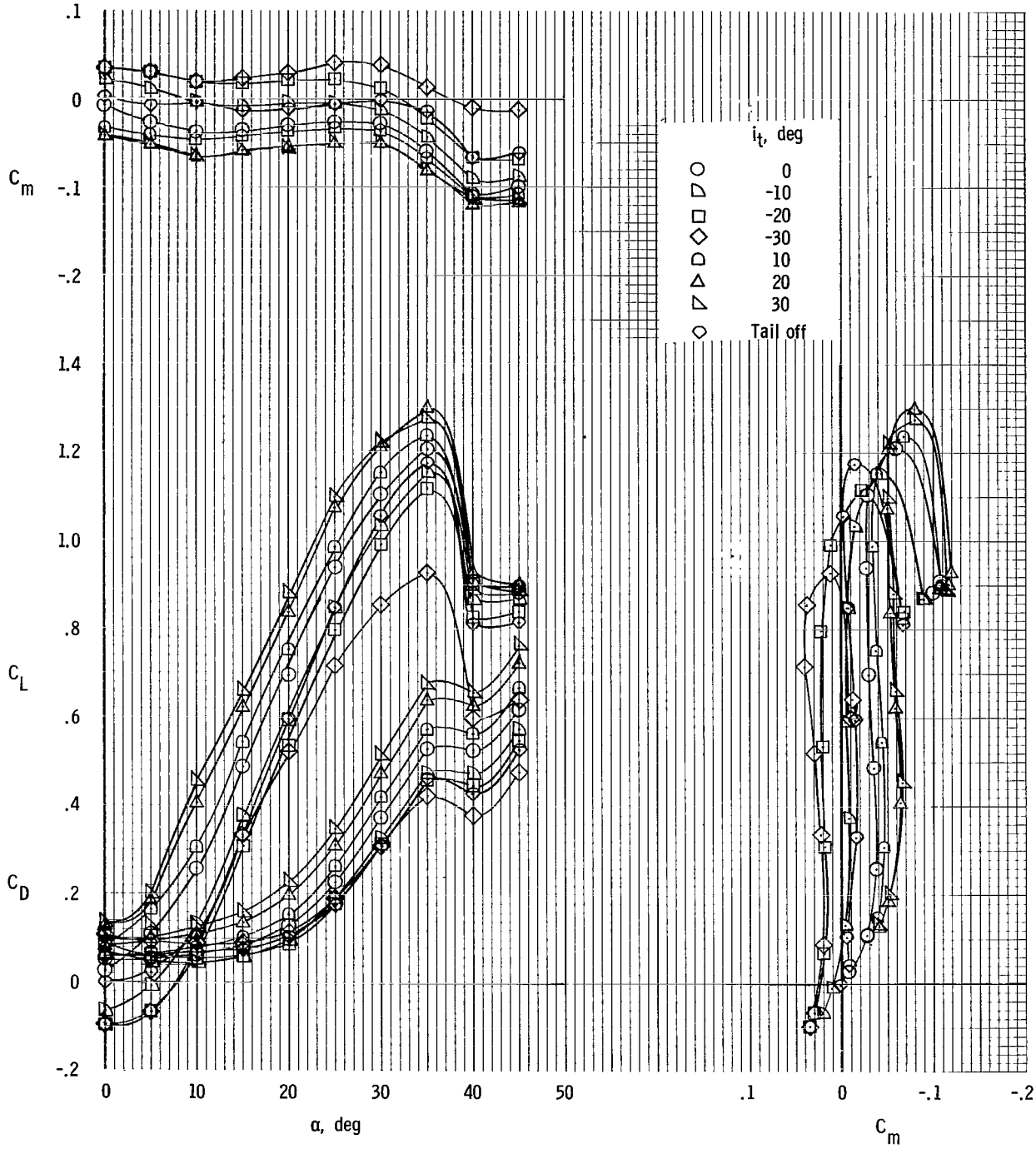

(c) Horizontal control surface.

Figure 11.- Concluded.

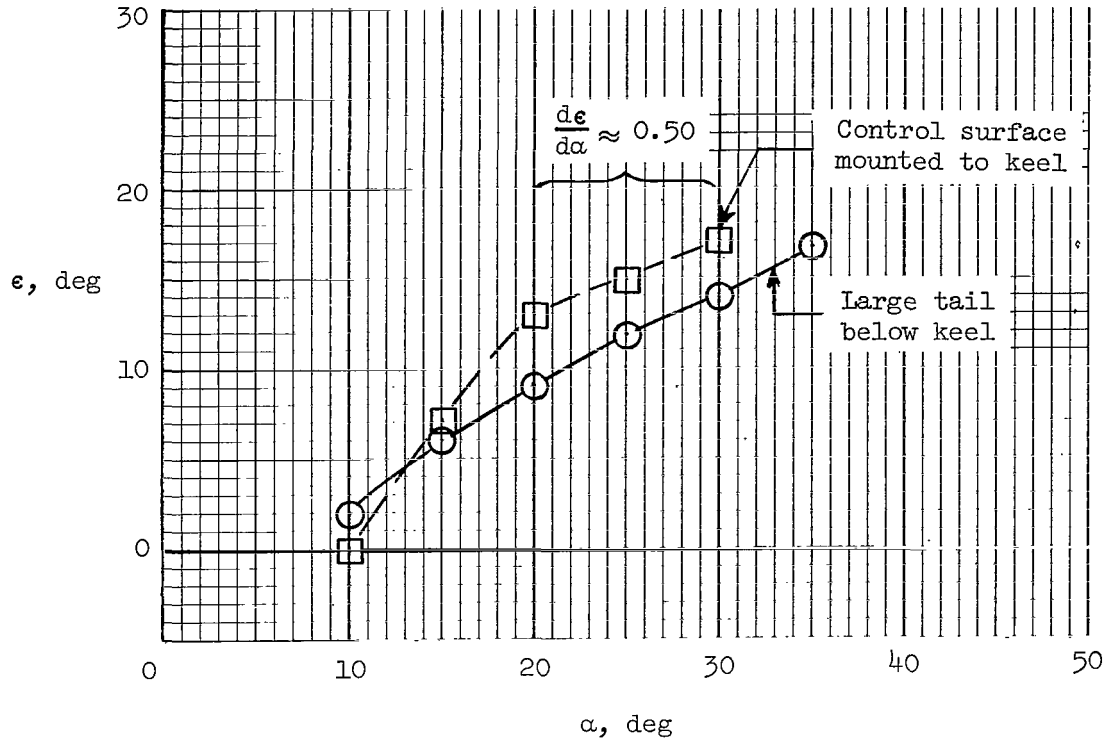

Figure 12.- Variation of downwash angle with angle of attack for large horizontal tail below keel and horizontal control surface mounted to keel. (Data derived from figs. 11(b) and 11(c).)

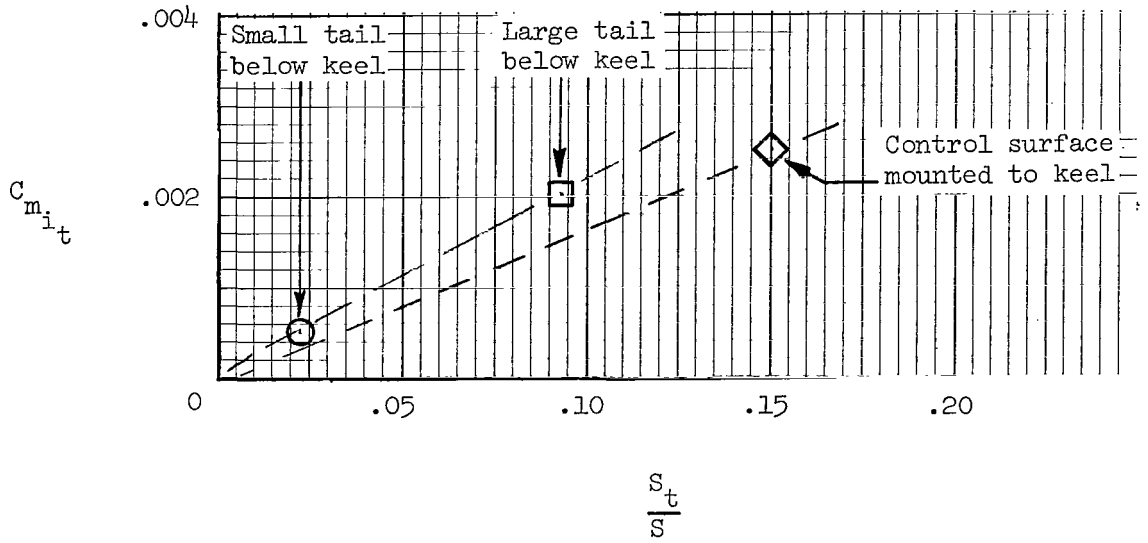

Figure 13.- Variation of horizontal control surface effectiveness with tail size for the configuration investigated.

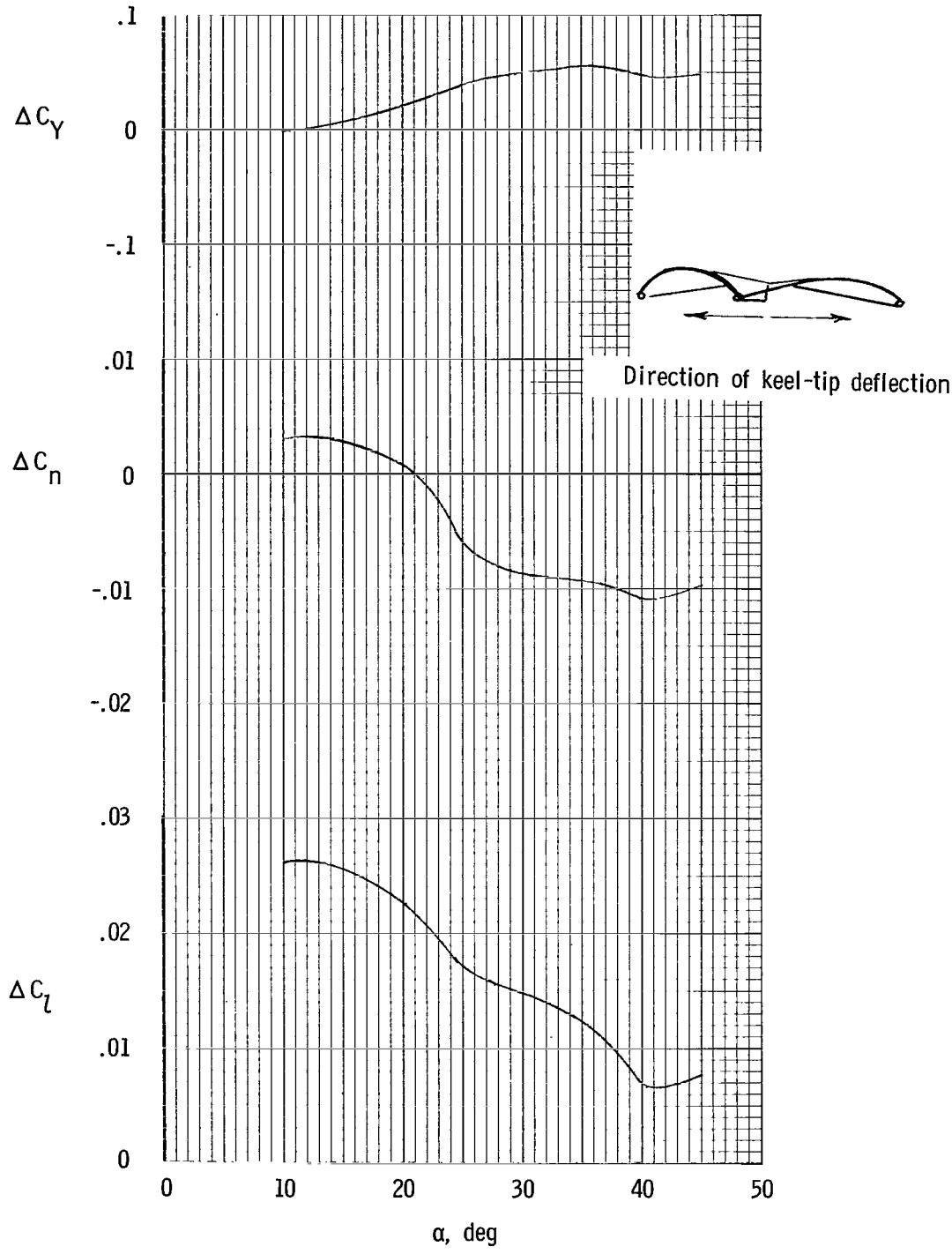

Figure 14.- Incremental lateral control force and moments produced by lateral deflection of the keel trailing edge. Force-test model. $\delta_t = \pm 20^\circ$.

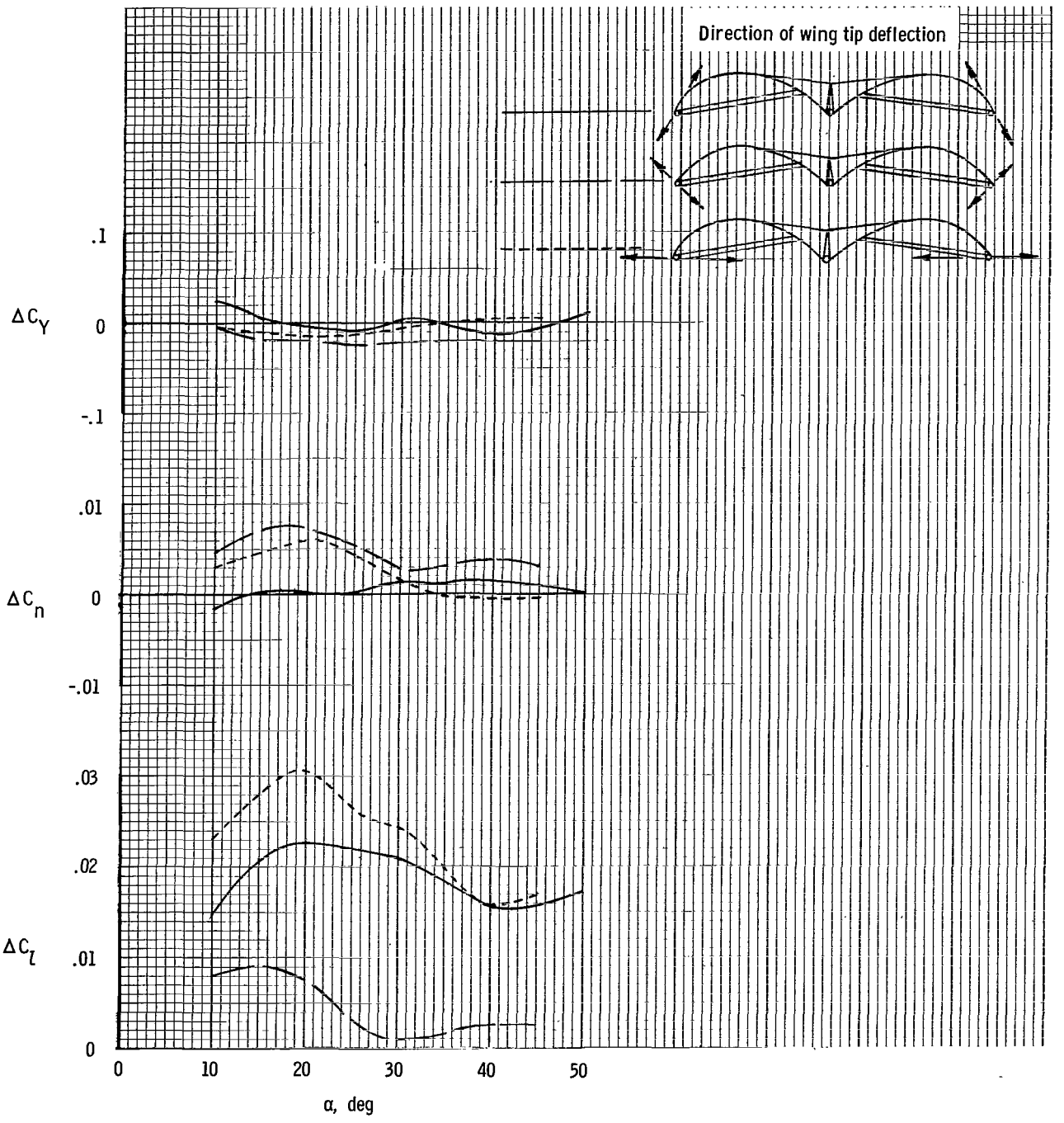

Figure 15.- Incremental lateral forces and moments produced by deflection of the wing tips in various directions. $\delta_t = \pm 20^\circ$. Force-test model.

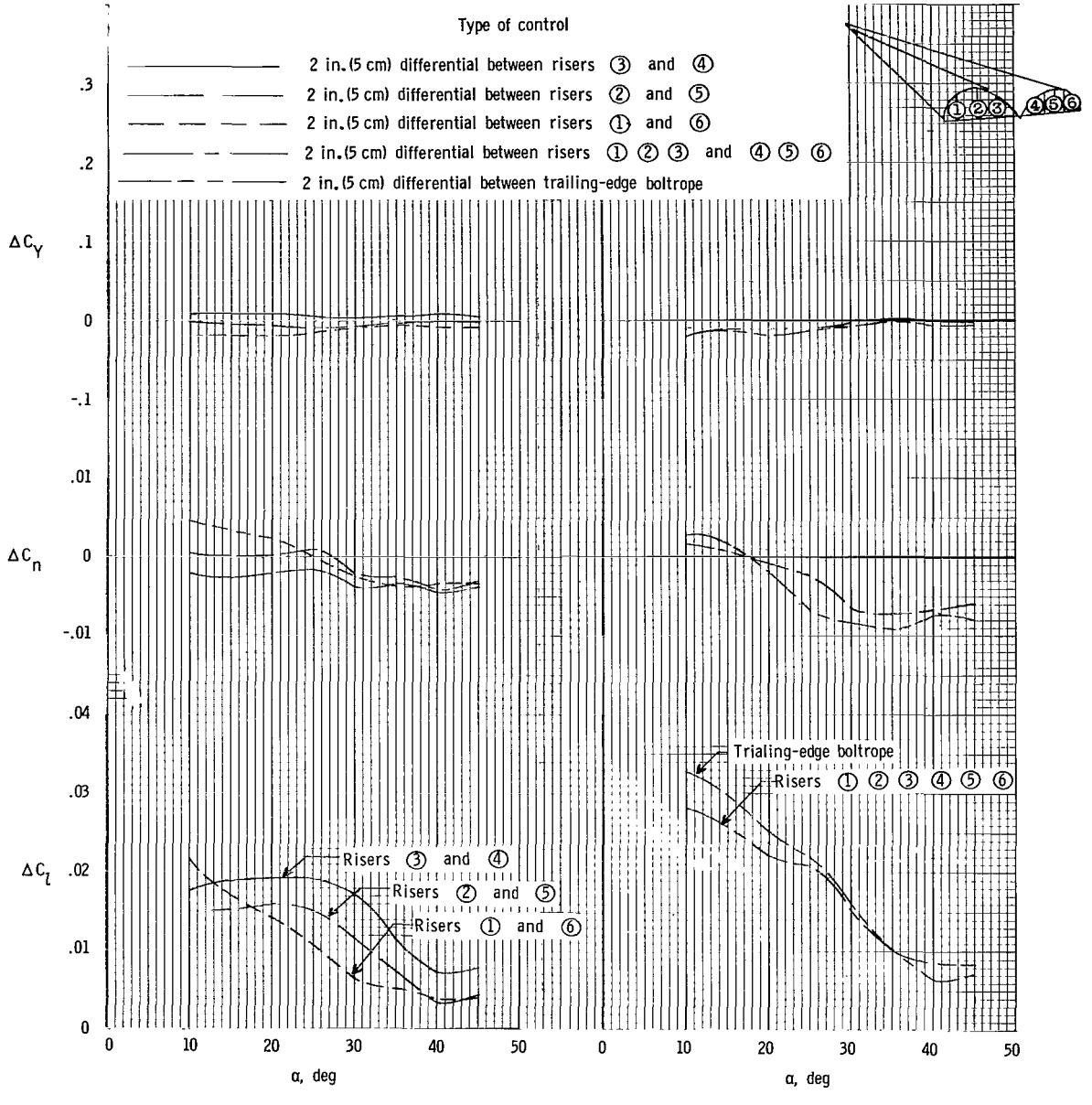

Figure 16.- Incremental lateral control force and moments produced by differential deflection of trailing-edge risers and by differential deflection of boltrope control. Force-test model.

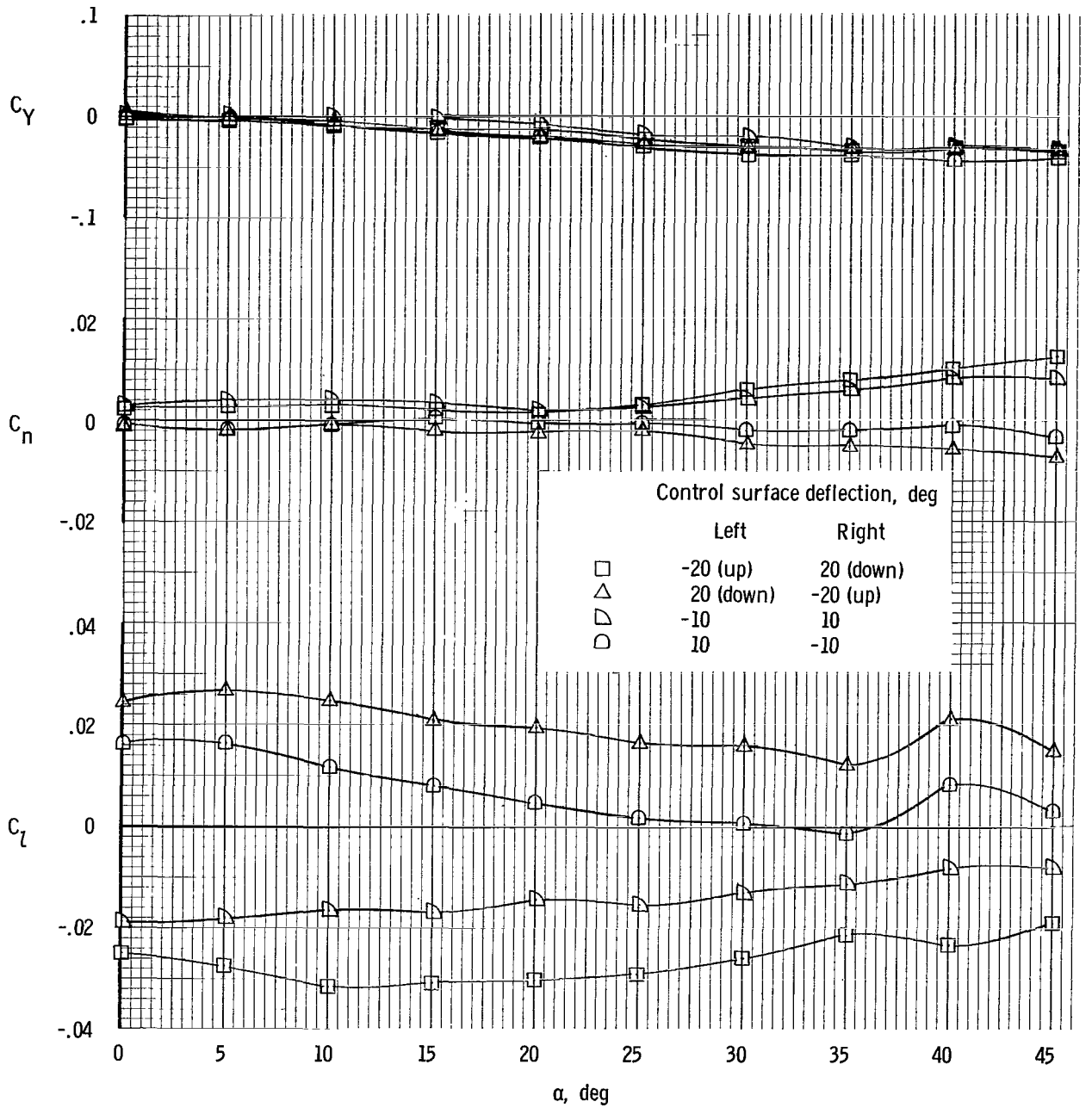

(a) Force and moment coefficients.

Figure 17.- Lateral control characteristics produced by differential deflection of horizontal control surface. Force-test model.

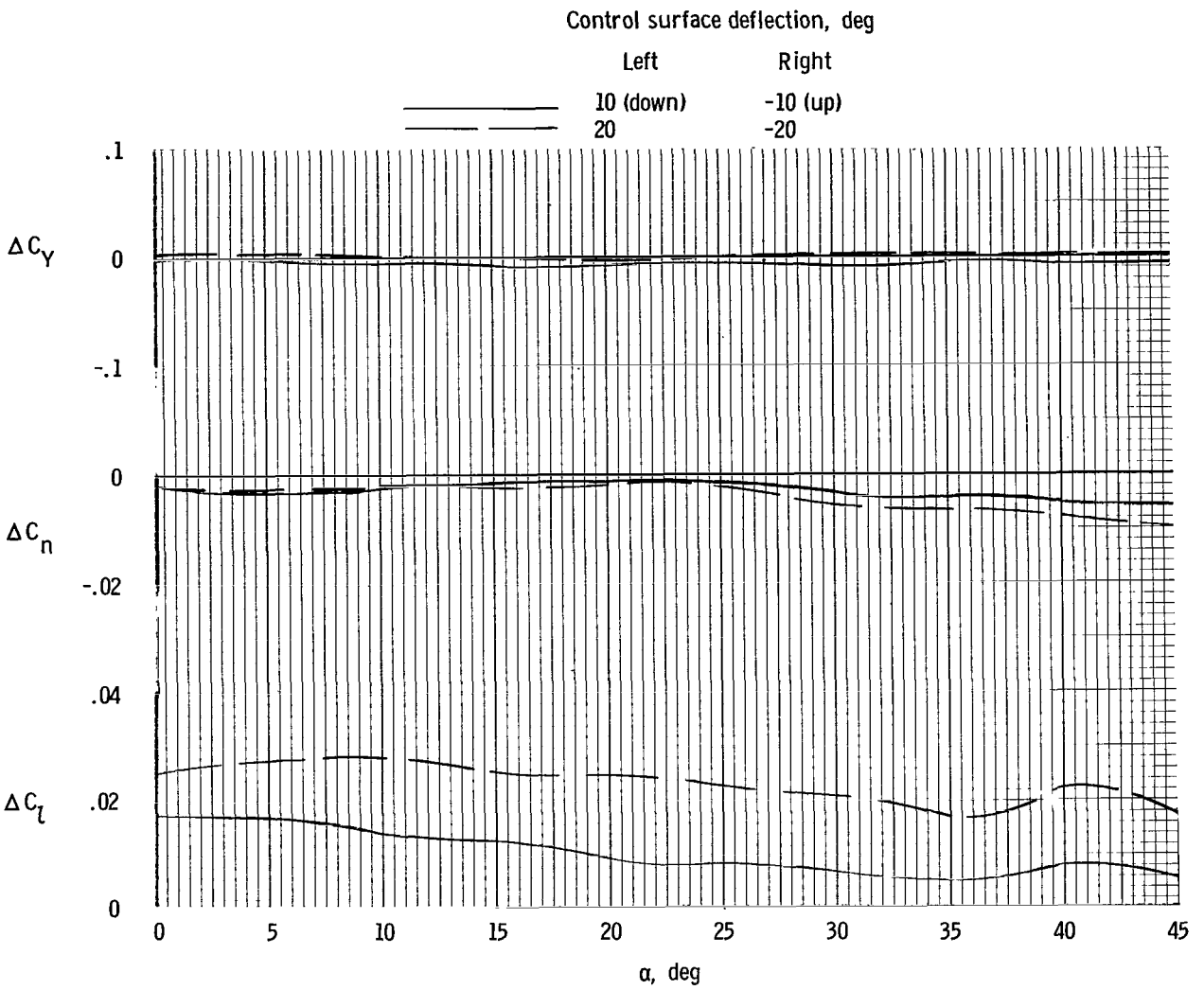

(b) Incremental lateral force and moment coefficients.

Figure 17.- Concluded.

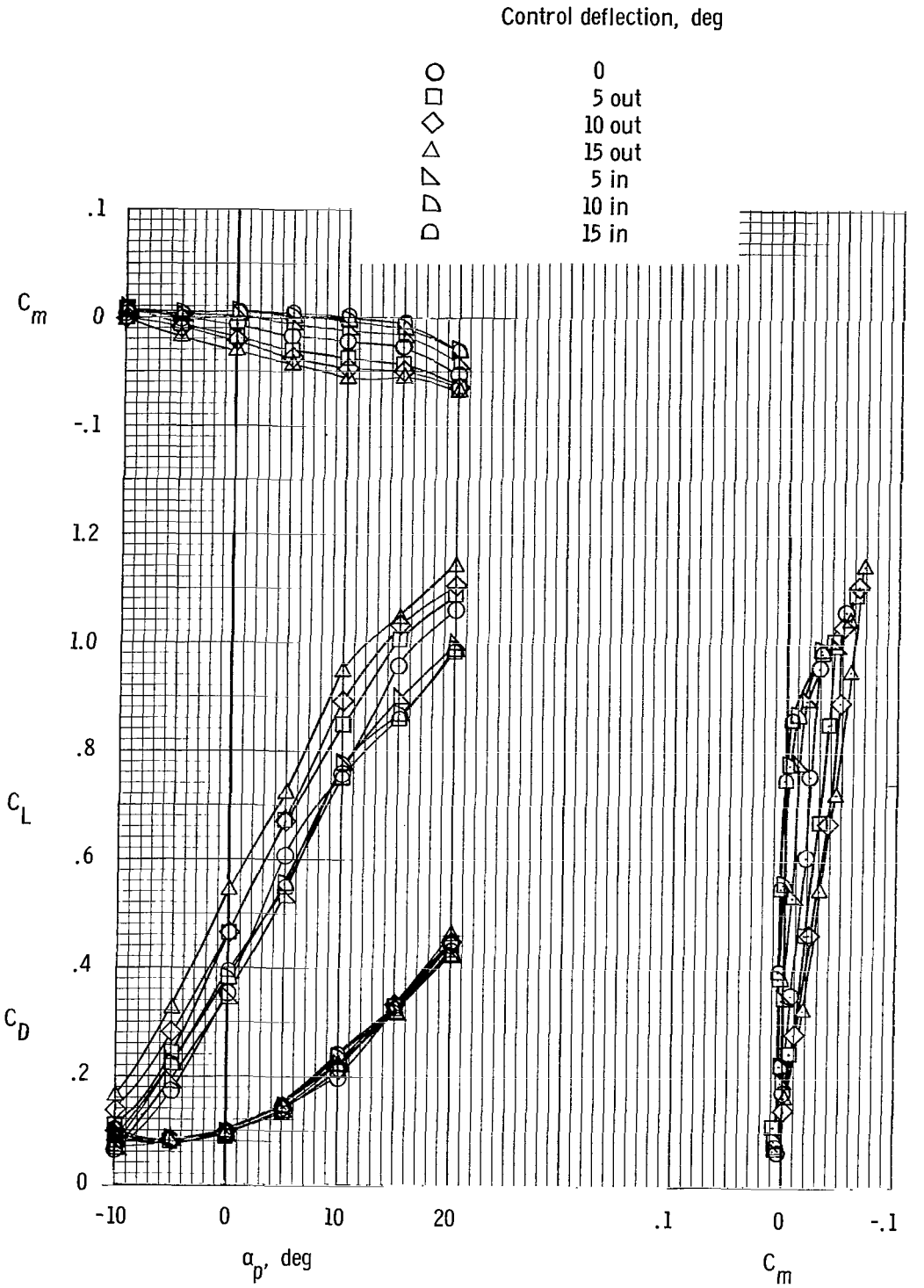

Figure 18.- Effect of wing-tip deflection on the longitudinal characteristics of the flight-test model. $i_w = 20^o$.

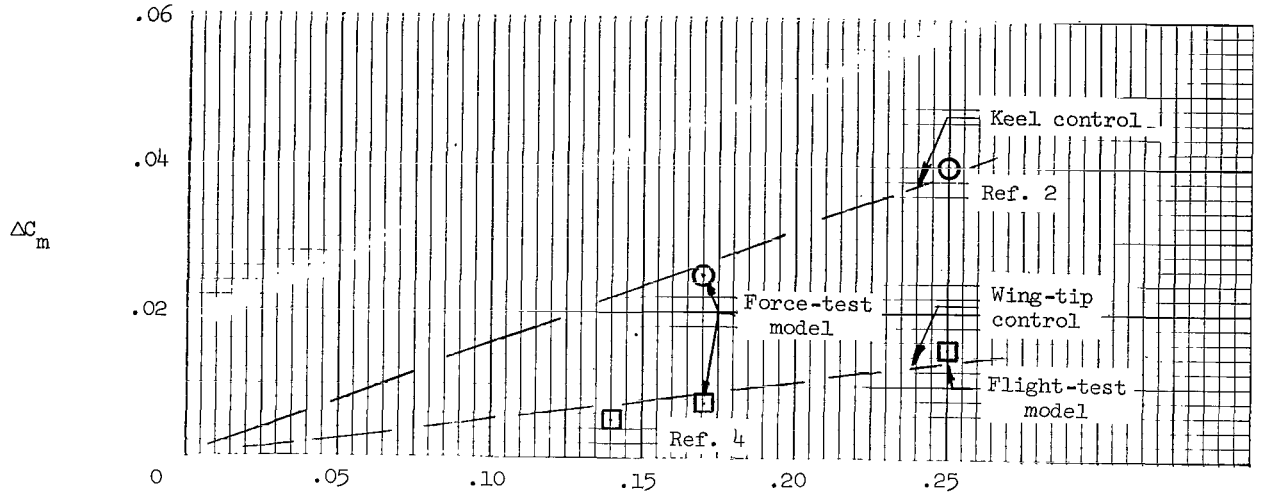

Ratio of control length to leading-edge length.

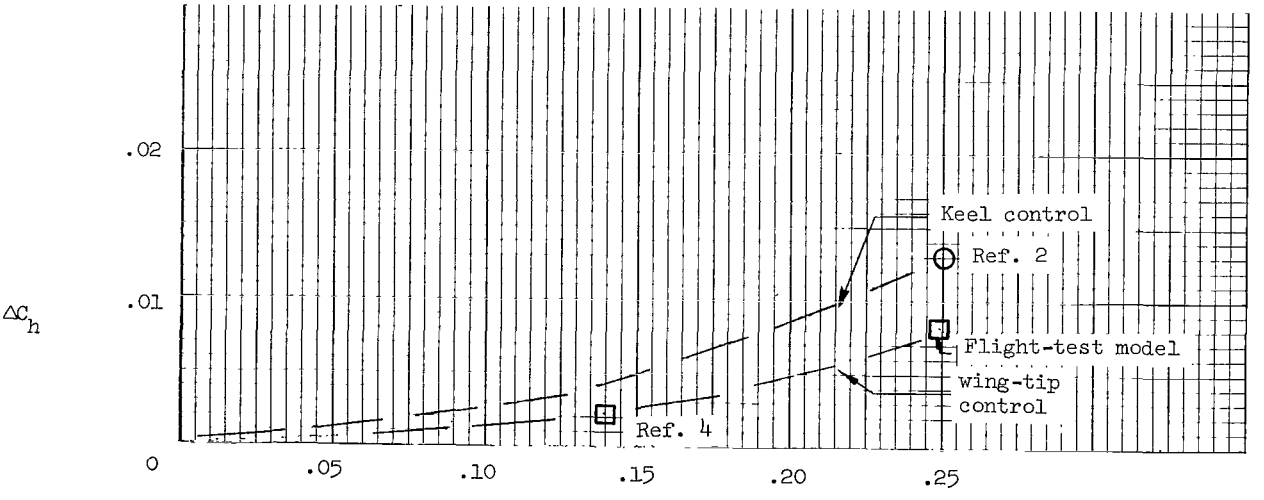

Ratio of control length to leading-edge length.

Figure 19.- Variation of incremental pitching-moment and hinge-moment coefficients with tip length for keel-control and wing-tip-control systems. Data presented for control deflections of ±5°. $\alpha_k = 20°$.

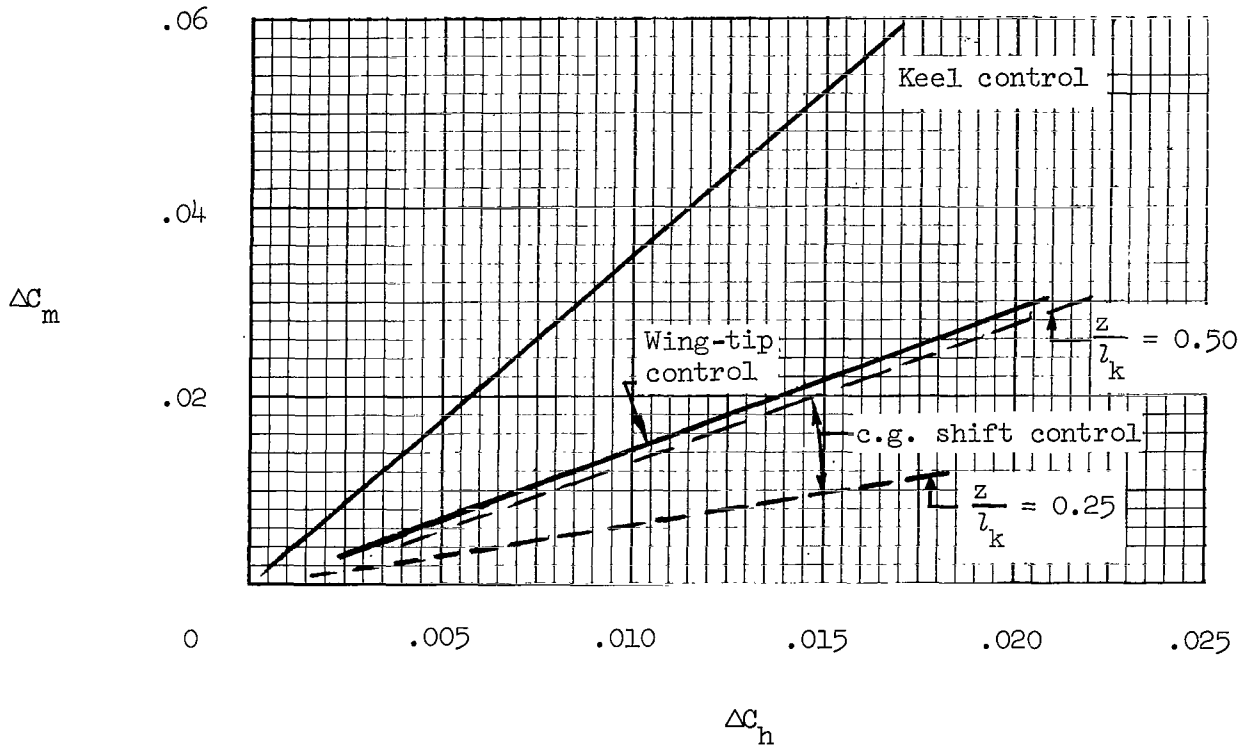

Figure 20.- Variation of incremental pitching-moment coefficient with incremental hinge-moment coefficient for several different longitudinal control systems. $\alpha_k = 20^\circ$.

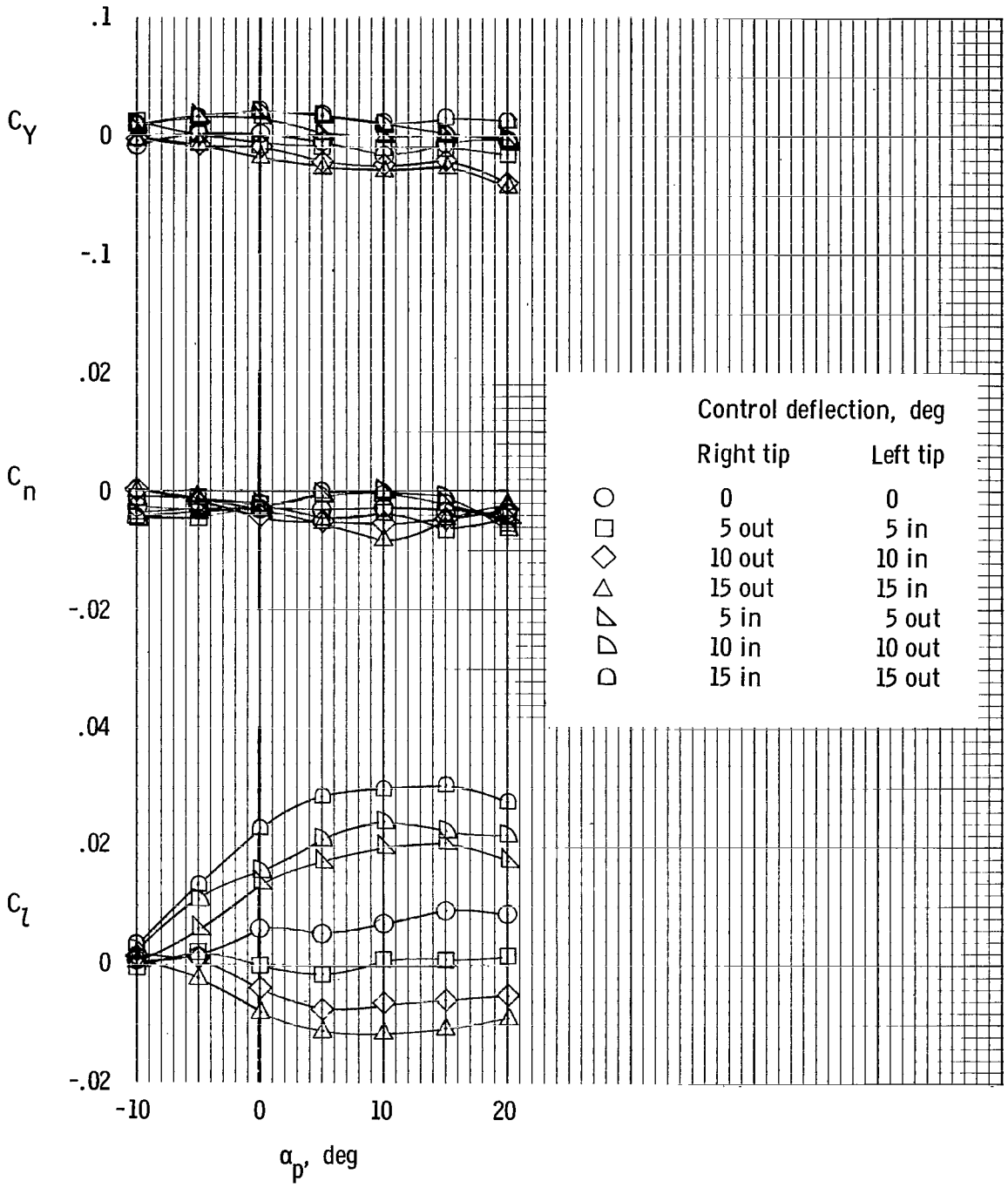

(a) Force and moment coefficients.

Figure 21.- Lateral control characteristics produced by deflection of wing tips on the flight-test model. $i_w = 20^o$.

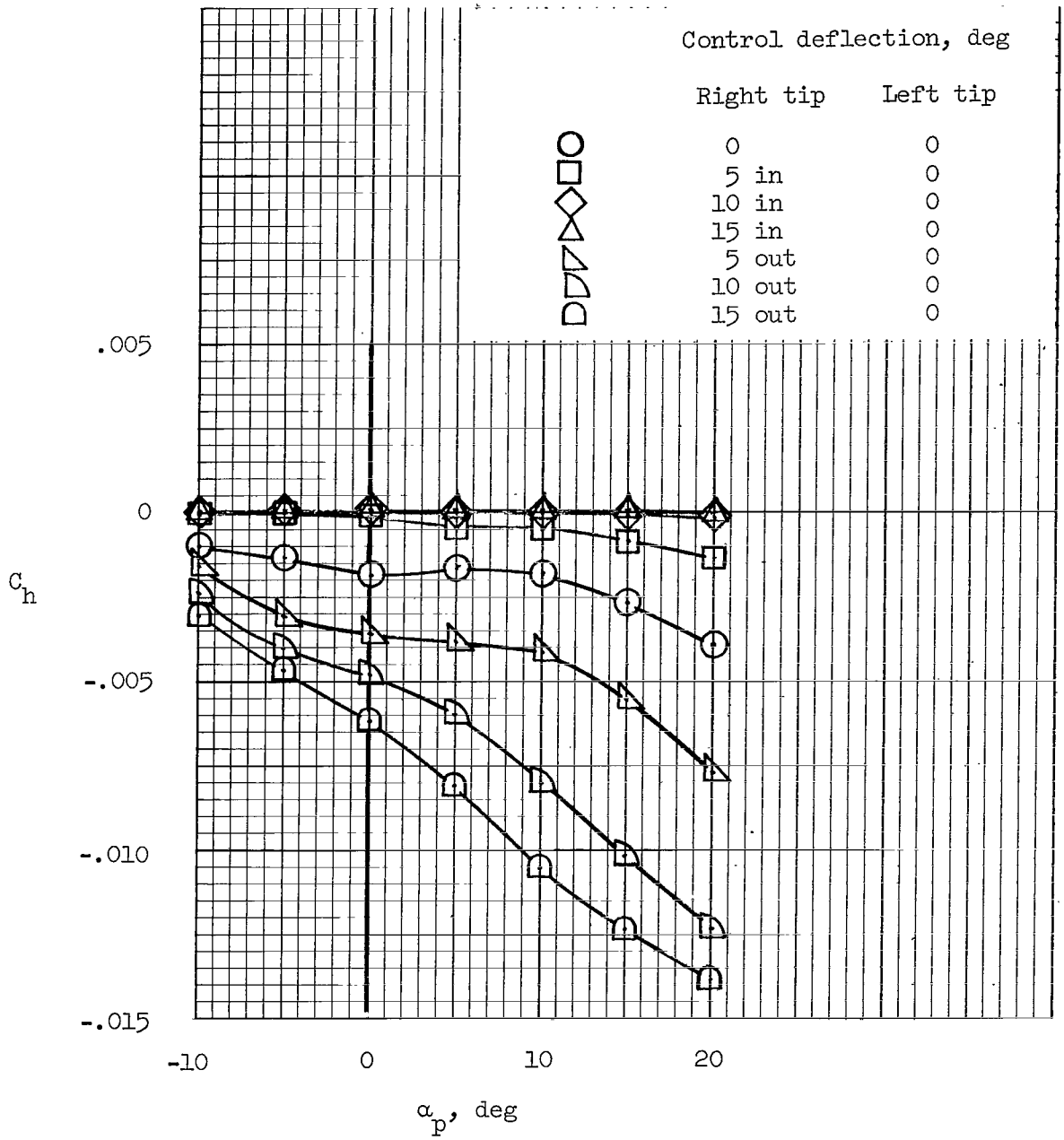

(b) Hinge-moment coefficients.

Figure 21.- Continued.

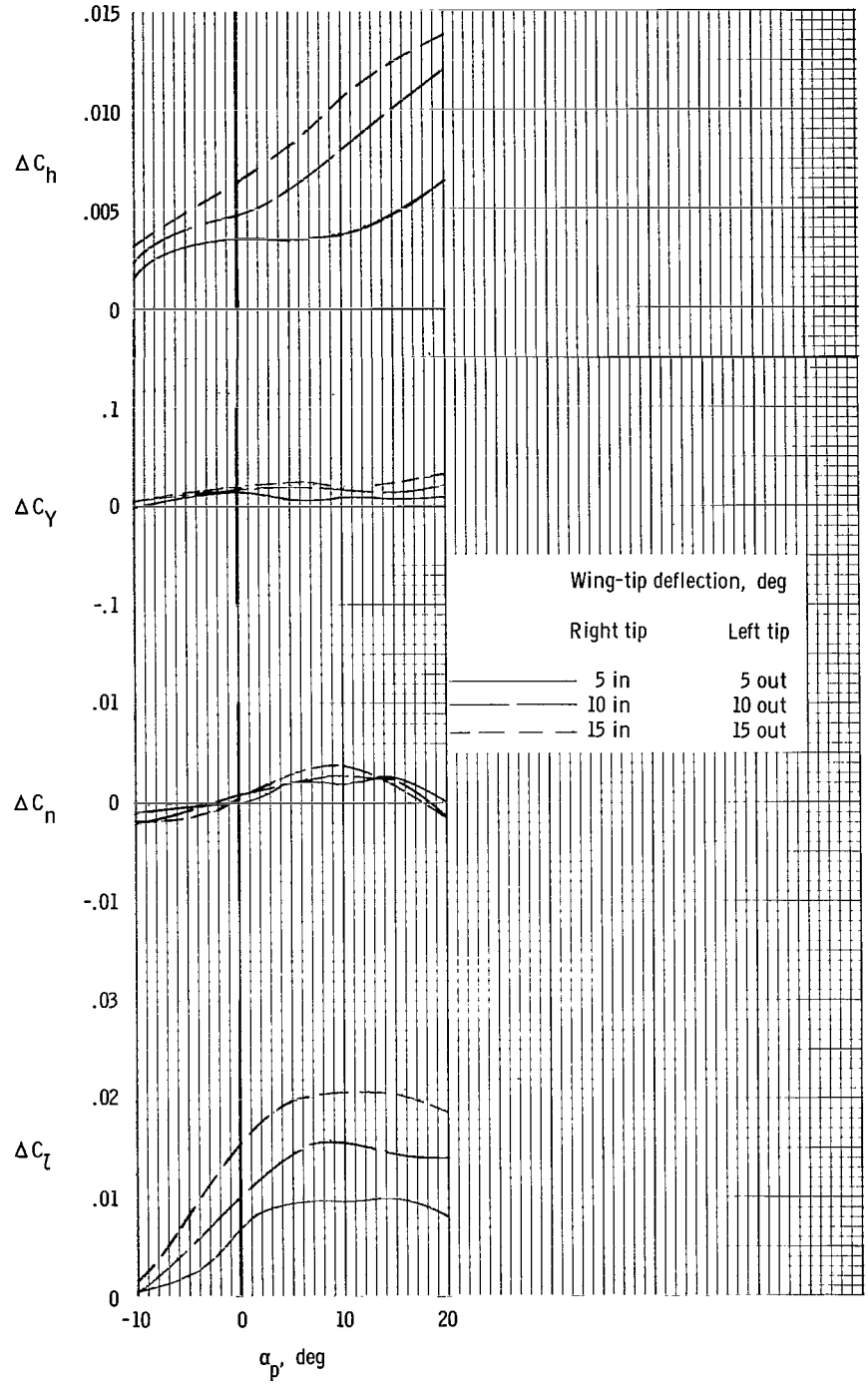

(c) Incremental lateral force and moment coefficients.

Figure 21.- Concluded.

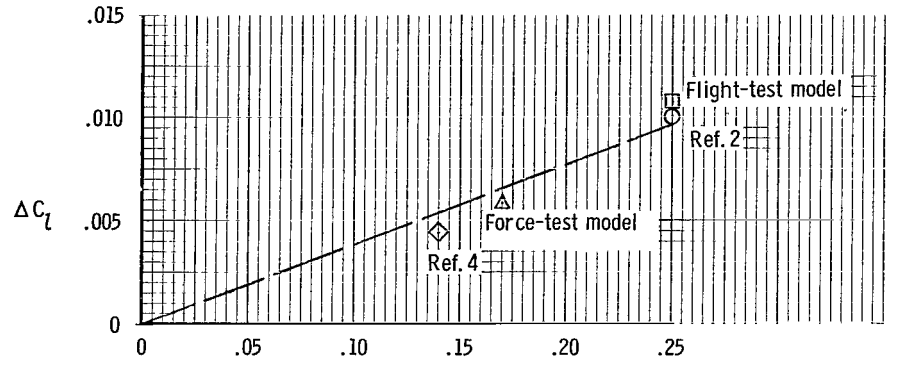

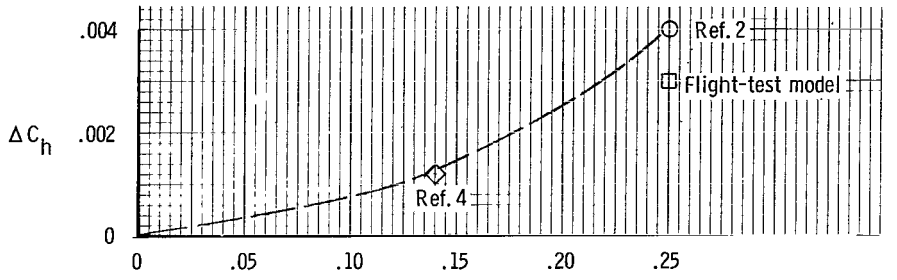

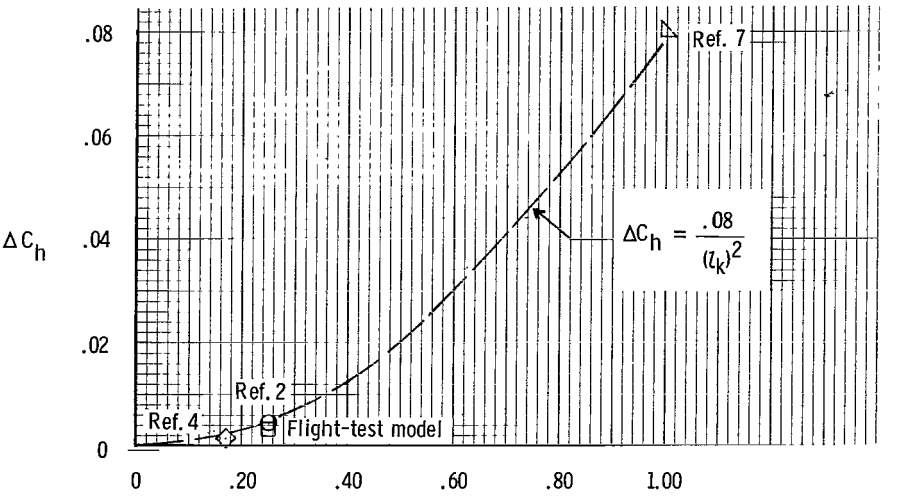

Figure 22.- Incremental rolling- and hinge-moment coefficients produced by wing-tip deflection. Data presented for deflections of ±5°. $\alpha_k = 25°$.

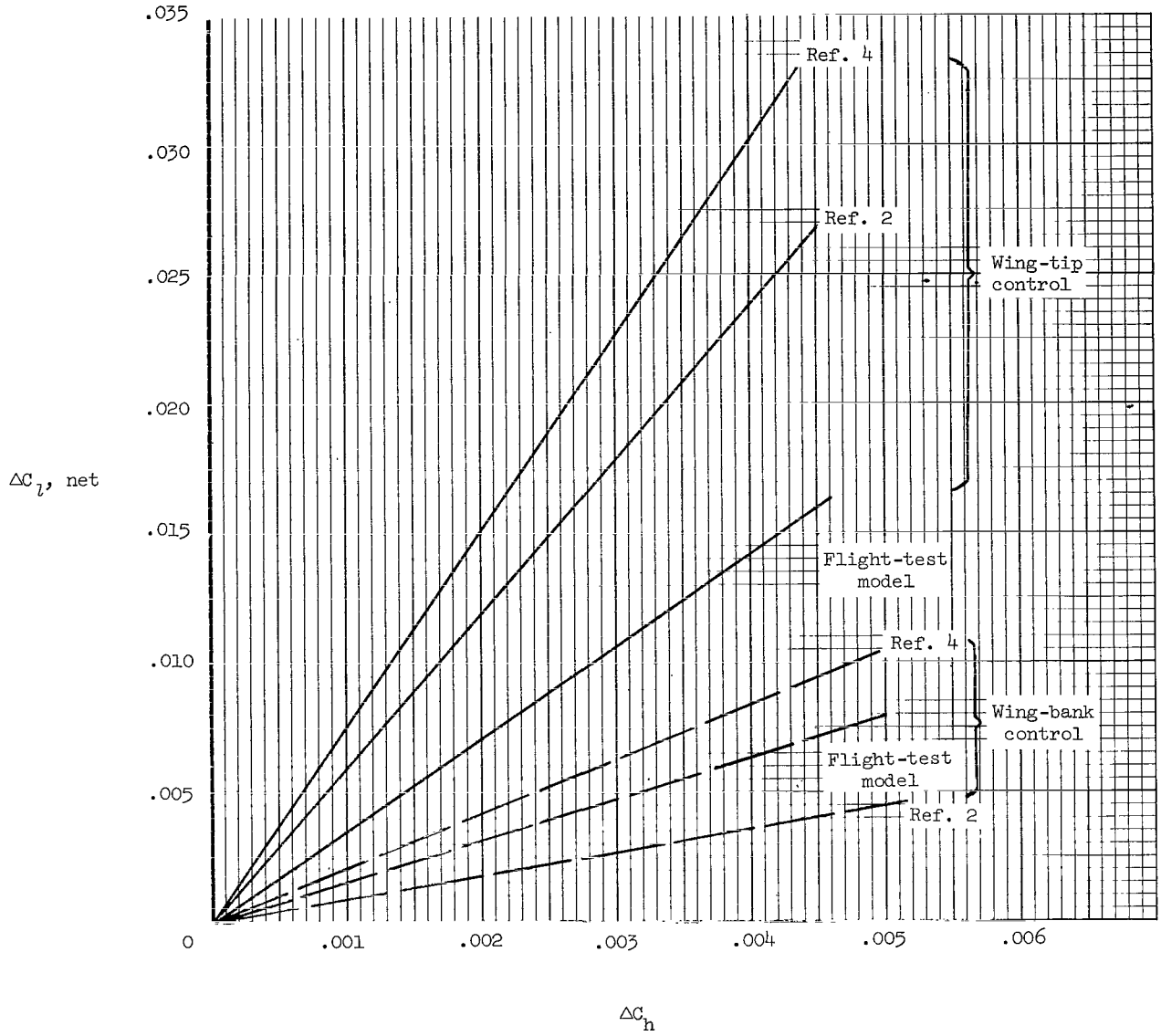

Figure 23.- Comparison of the lateral characteristics of the wing-bank control system with the lateral characteristics of the wing-tip control system for three different parawing configurations. $\alpha_k = 25^\circ$.

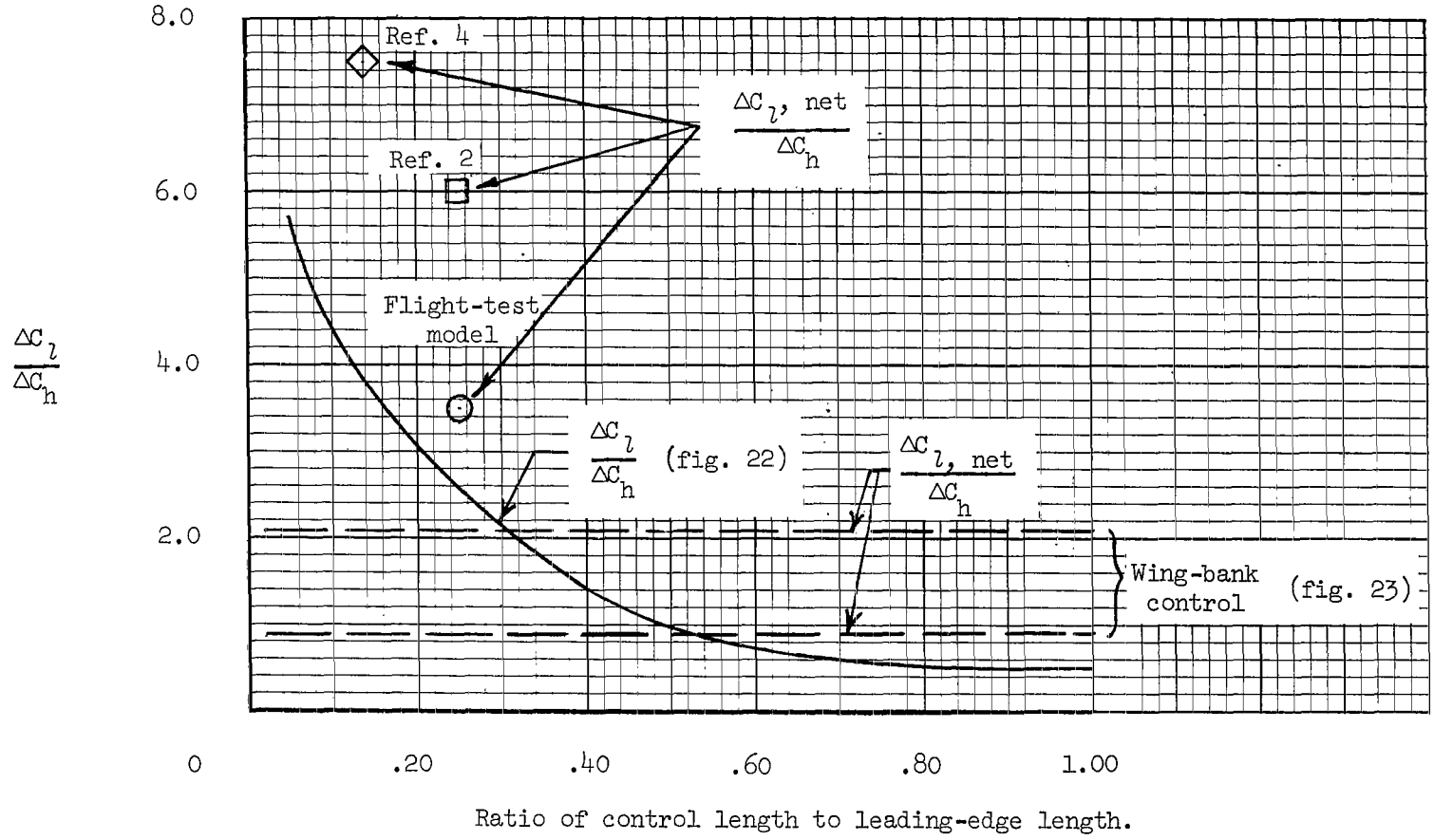

Figure 24.- Comparison of the ratio of incremental rolling moment to hinge moment with the ratio of tip length to keel length for several different parawing configurations employing the wing-tip and wing-bank control systems. $\alpha_k = 25^\circ$.

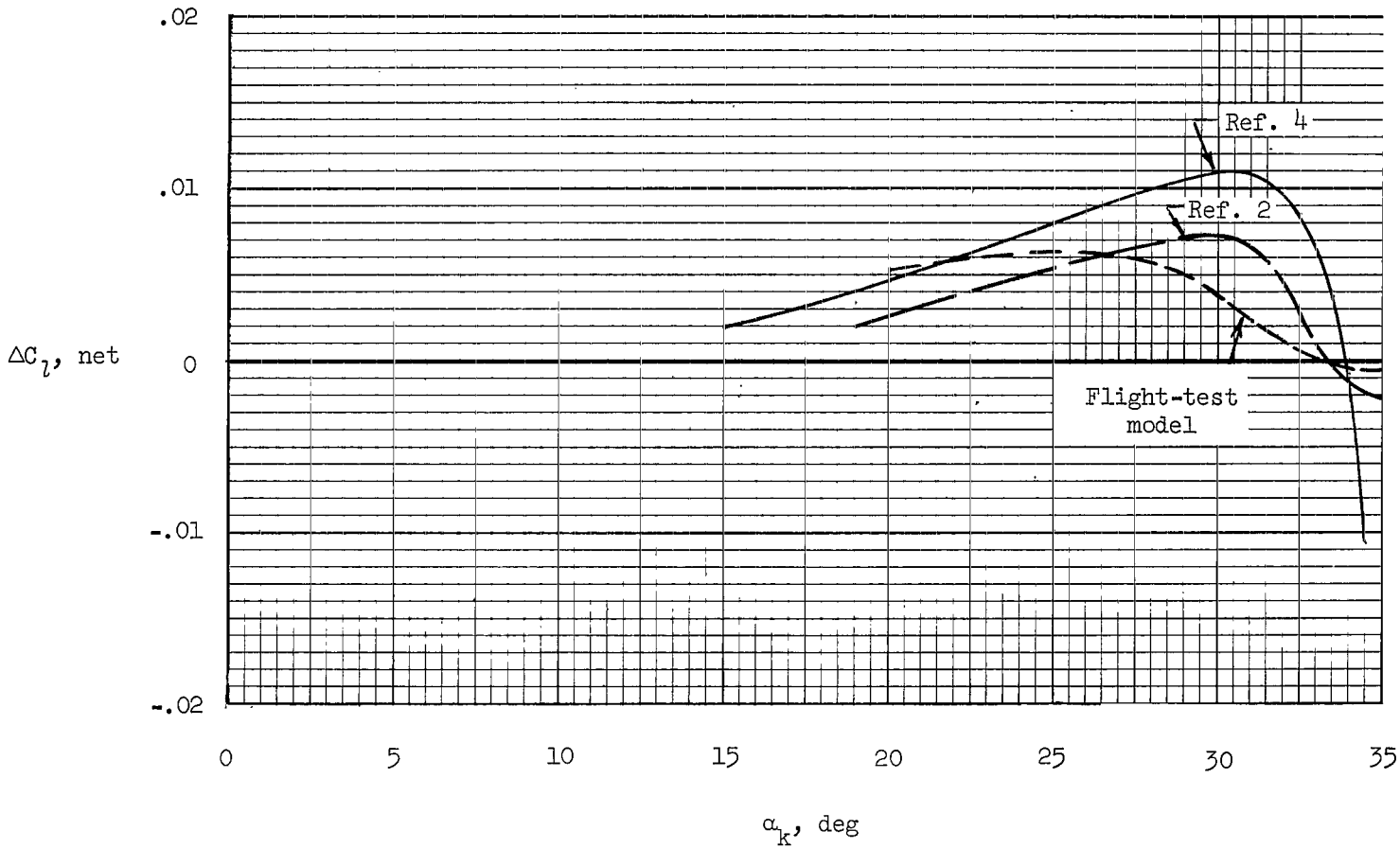

Figure 25.- Calculated incremental net rolling-moment coefficient produced by 5° of wing bank for three different parawing configurations.

A motion-picture film supplement L-882 is available on loan. Requests will be filled in the order received. You will be notified of the approximate date scheduled.

The film (16 mm, 4 min, color, silent) deals with a low-speed flight investigation of a model of a parawing utility vehicle. Flight tests were made over an angle-of-attack range of the parawing keel from about 23° to 38° and control was achieved through deflection of hinged wing tips.

Requests for the film should be addressed to:

Chief, Photographic Division
NASA Langley Research Center
Langley Station
Hampton, Va. 23365

C U T

Date _____

Please send, on loan, copy of film supplement L-882 to TN D-2998.

_____
Name of organization

_____
Street number

_____
City and State Zip code

Attention: Mr. _____

Title _____

3/18/85

"The aeronautical and space activities of the United States shall be conducted so as to contribute . . . to the expansion of human knowledge of phenomena in the atmosphere and space. The Administration shall provide for the widest practicable and appropriate dissemination of information concerning its activities and the results thereof."

—NATIONAL AERONAUTICS AND SPACE ACT OF 1958

NASA SCIENTIFIC AND TECHNICAL PUBLICATIONS

TECHNICAL REPORTS: Scientific and technical information considered important, complete, and a lasting contribution to existing knowledge.

TECHNICAL NOTES: Information less broad in scope but nevertheless of importance as a contribution to existing knowledge.

TECHNICAL MEMORANDUMS: Information receiving limited distribution because of preliminary data, security classification, or other reasons.

CONTRACTOR REPORTS: Technical information generated in connection with a NASA contract or grant and released under NASA auspices.

TECHNICAL TRANSLATIONS: Information published in a foreign language considered to merit NASA distribution in English.

TECHNICAL REPRINTS: Information derived from NASA activities and initially published in the form of journal articles.

SPECIAL PUBLICATIONS: Information derived from or of value to NASA activities but not necessarily reporting the results of individual NASA-programmed scientific efforts. Publications include conference proceedings, monographs, data compilations, handbooks, sourcebooks, and special bibliographies.

Details on the availability of these publications may be obtained from:

SCIENTIFIC AND TECHNICAL INFORMATION DIVISION

NATIONAL AERONAUTICS AND SPACE ADMINISTRATION

Washington, D.C. 20546